Sonic sands

Bruno Andreotti

Physique et Mécanique des Milieux Hétérogènes, UMR 7636 ESPCI -CNRS, Univ. Paris-Diderot, 10 rue Vauquelin, 75005 Paris, France

Abstract
Many desert sand dunes emit a loud sound with a characteristic tremolo around a well-defined frequency whenever sand is avalanching on their slip face. This phenomenon, called the 'song of dunes', has been successfully reproduced in the lab, on a smaller scale. In all cases, the spontaneous acoustic emission in air is due to a vibration of the sand, itself excited by a granular shear flow. This review presents a complete characterization of the phenomenon—frequency, amplitude, source shape, vibration modes, instability threshold—based on recent studies. The most prominent characteristics of acoustic propagation in weakly compressed granular media are then presented. Finally, this review describes the different mechanisms proposed to explain booming avalanches. Measurements performed to test these theories against data allow one to contrast explanations that must be rejected—sound resonating in a surface layer of the dune, for instance—with those that still need to be confirmed to reach a scientific consensus—amplification of guided elastic waves by friction, in particular.

(Some figures may appear in colour only in the online journal)

Contents

*'Sur la plage le sable bêle
Comme des moutons d'infini
Quand la mer bergère m'appelle'*
Leo Férré, La mémoire et la mer[1]

1. Introduction

1.1. A history of wilderness

A land of dissonance. If there was an absolute need for finding a mystery of the Sahara, we would propose the contrast between the void of this zone and the multiplicity of its interpretations. Despite the number of meticulous studies devoted to various aspects of the great African desert (ranging from Berber linguistics to pre-Islamic art and from tribal rites to geography), images have remained blurred as if academic knowledge was tricked by imagination. While rational analysis has failed to fill up the virgin space of the desert, literature has transformed it into an organic and mythical universe, populated by fantasy and irrationality. Analysing the historical accounts of booming sand dunes, the reader actually discovers that this apparent dissonance between erudite and literary imaginaries hides connections—and even probably a connivance—between the knowledge of scientists, the programs of politicians and the visions of writers [106].

A colonial perspective on booming sand dunes. Most reports of singing sands date back to the colonial period (figure 1) and were written by travellers (e.g. Burton [25], Doughty [40], Harding King [53] and Thomas [101]), military explorers (e.g. Goldsmid [48], Shaw [97] and Bagnold [8]) and scholars (e.g. Darwin [36], Bollaert [15] and Lenz [69]), with a special mention of the review written by Curzon, Viceroy of India [32]. The texts share a similar structure. The geography of the site is usually detailed and the acoustic emission is described using a musical analogy—for instance, 'It is simply a bed of loose sand on the slope of the hill, which, if set in motion by any cause, as by the wind or a man rolling down from the top, produces lengthened sonorous vibrations not unlike those of the string of a bass viol' [32]. The most frequently invoked instruments are trumpets, which have a rich timbre like bass viols, and, more surprisingly, percussion instruments like drums (naqaras in particular). With striking systematism, the rationalism of the traveller is contrasted with the fears and the superstitions of the 'ignorant' natives who, 'of course, ascribe miraculous properties to the (sand) hill' [32]. In Afghanistan, 'he would be a bold man who tried to explain the (phenomena) by natural causes within a hundred miles of its influence' [32]. In Peru, the natives 'started to explain in chorus that the sandhill (...) was haunted, and that the dead Indians of the gentilar danced every night to the beating of drums' [105]. In Hawaii, 'the small fishing boats, when the wind allows them, prefer to pass off this coast: it comes from the white extent a strange moaning, a complaint, like the howl of a dog, that the natives attribute to restless spirits' [68]. This construction of colonial exoticism finds its quintessence in

fiction: 'Somewhere, near us, in an undefined direction, a drum was beating, the mysterious drum of the dunes; it was beating distinctly, at first vibrating loudly, then more feebly, stopping, then taking up its fantastic bearing again. The Arabs, terrified, looked at one another; and one said in his own language: "Death is upon us". Just then, suddenly, my companion, my friend, almost my brother, fell on his head from his horse, struck down ahead by a sunstroke' [74].

A sterile area, mother of the truth. Meetings with people living in the neighbourhood of booming dunes in the Atlantic Sahara have led us to hypothesize that the relation of a desert to transcendence is mostly a Christian construction. It is particularly striking that the word 'desert', ubiquitous in the Bible, does not appear in the Qur'an. In the Bible, wilderness is the virgin playground where Good ('I'm a voice crying out in the desert: Make the way for the Lord straight' John 1 : 23) and Evil ('So if they say to you, "Behold, the Messiah is in the desert," do not go out' Matthew 24 : 26; 'When an evil spirit comes out of a man, it goes into the desert seeking rest and does not find it' Matthew 12 : 43, Luke 8 : 29, Luke 11 : 24) clash. For the Puritans that settled in New England, this double symbolic system became a dialectic between wandering in the wilderness [75] and city foundation. Pétillon even suggests that this theme underlies all of American literature, which seems obsessed by the question: 'What went ye out into the desert to see? A reed shaken with the wind?' (Matthew 11 : 7) [88].

Cross, subdue, occupy and exploit. Historical texts on singing sands therefore suggest an interaction between exotic imaginary and learned studies at all stages of the desert colonization process, from the first explorers to the exploitation of natural resources [106]. The conquest by Science escorts that by weapons, and rounds it off. The exotic fantasy redoubles itself through the scientistic myth of a desert under the control of technology. Analysing news with this interpretive lens shows that it may still be relevant today.

1.2. Booming dunes as scientific objects

Methodology. In the last few decades, singing sands have become a highly controversial scientific topic, with a remarkably low rate of convergence towards scientific consensus [10]. Not only the sound emission mechanism but also the most elementary observations are still debated. Although positivism is not exempt from problems, it seems likely that the controversies about singing sands can only be resolved within the scientific discipline, by considering only self-consistent, refutable hypotheses and theories. Therefore, this review will first examine problems and statements that seem unfalsifiable—i.e. for which one cannot conceive any physical experiment that could show that they are false— and thus, according to K Poppers, non-scientific. This of course does not preclude relevance or interest. Along the same line, it seems necessary to hold-off statements with exotic connotations concerning the supposed 'mysteries' of booming dunes. The rest of the review will focus on consensual facts, arguments, models and possible tests to corroborate or refute

---

[1] *'On the beach sand bleats
Like sheep of infinity
When the sea shepherdess calls me'.*

Figure 1. Top: (left) The Tun Huang Lu manuscript (9th century), brought back by Sir Aurel Stein from Tunyang, describes the Ming-sha-shan site (China). Copyright, the British Library Board 2011[2]. (Right) Marco Polo [89]. Middle: (left) the Mughal emperor Babur (from the National Museum, New Delhi) and (middle) Odoric of Pordenone [111] evoke Reg-i-Ruwan (Afghanistan). (Right) Map of the North Western part of the Rub' Al Khali established by Charles Montagu Doughty [40]. Bottom: photographs of four of the most famous travellers who referred to singing sands. From left to right: Bertram Thomas became the first European to cross the Rub' Al Khali [101]; (middle left) Harry St John Philby, whose mission during WWI was to organize the Arab Revolt against the Ottoman Empire [92]; Ralph Bagnold, who first crossed the Lybian desert during his active duty in the Royal Engineers [8, 9]; George Nathaniel Curzon, First Marquess Curzon of Kedleston, Viceroy of India [32].

hypotheses. Whenever consensus is not reached, the level of agreement on test results will be given, based on the literature.

A first description of singing sands. Many desert sand dunes emit a loud and harmonious sound as they avalanche, with large amounts of sand sliding down their slip faces. The acoustic emission is really a sound whose energy is concentrated around a well-defined frequency and its harmonics, and not a broadband noise [31, 32, 82]. If, instead of using gravity, a sand shear flow is driven by the motion of a solid body (pushing sand with a blade, with hands or with the bottocks), an acoustic emission occurs as well, but at a different frequency [50]. The sound is emitted in air by the vibration of the sand free surface, which plays the role of a loud-speaker membrane [4].

Triggering of avalanches. The booming results from the granular motion and is thus not directly due to the wind. The effect of the air flow is only to transport sand on the stoss slope of the dune and to accumulate it at the top of the slip face. When the slope becomes locally larger than the static friction coefficient $\mu_s = \tan(\theta_s)$, an avalanche spontaneously nucleates and propagates down the dune. The flow stops when the slope has relaxed everywhere below the dynamic friction coefficient $\mu_d = \tan(\theta_d)$. θ_s and θ_d are, respectively, around 35° and 31° for natural aeolian sand. Frequently, the propagation of a booming avalanche triggers dynamically another avalanche at a different place of the dune slip face, which can emit sound as well. Finally, an avalanche can be triggered and fed by a man-made slide. When the human slider does not beat his legs or his buttocks, the avalanche remains homogeneous and steady, and shares the same characteristics as spontaneous ones.

1.3. Scientific issues

As mentioned earlier, we wish in this review to focus on problems and hypotheses that can be tested experimentally. However, a significant part of the literature has focused on three problems that we consider to be ill-posed. By that we mean their formulation is responsible for the controversy that they generate. They therefore cannot be closed. Even though these questions may be interesting, they tend to pollute the scientific debate and to delay the drawing up of common ground concerning the acoustic emission mechanism.

Are booming and squeaking the very same phenomenon? Humphries [55] has made the distinction between 'booming', used for the acoustic emission produced by an avalanche on a dune and 'squeaking', used for the sound emitted when one walks on certain beaches. By extension, Sholtz *et al* proposed the name 'squeaking' for the sound emitted from all types of granular shear flows except gravity-driven avalanches [98]. Although experiments [39, 50] have suggested a close connection between the two, Vriend, Hunt and co-workers at Caltech [56, 107, 108] claim that these two phenomena are fundamentally different in nature. Booming would need the resonance of a dune, which would be the equivalent of the sound box of an instrument, to get sustained emission. Squeaking, however, would consist of short bursts of sound when the sand is disturbed locally. Analysing in detail this utterance, one can identify the reason for which it can generate an endless controversy: it cannot be tested. Let us see how the machinery works on an example. Singing avalanches have now been reproduced in the lab, without any dune [34]. Whenever a given sand emits sound on a dune, it does the same in the lab and reciprocally. If one considers that booming is, by definition, a 'sustained' emission while squeaking consists of 'short' acoustic bursts, then laboratory shear flows are clearly booming as they can last for hours. Conclusion: laboratory scale and natural avalanches that emit sound share the same dynamical mechanisms and a resonance of the dune can be excluded. Counterargument: laboratory shear flows are not produced on the layered structure of a dune that could 'resonate'; they are thus not 'booming' [56]. Our own conclusion is that this question must be left aside, in order to progress in the understanding of the phenomenon. In this review, we will use the expressions 'booming', 'squeaking', 'whistling', 'song of dunes', 'acoustic emissions' and 'sonic' without making any prior difference of nature between the phenomena. At most, 'booming' will be more frequently used for low frequencies (on the order of 100 Hz) and 'squeaking' for high frequencies (on the order of 1 kHz).

What is so special about booming sand dunes? Previous reviews have listed the location of 40 booming sand dunes [56, 71]. Some dunes are known to sing when the sand is sufficiently dry; conversely, nobody has ever reported any acoustic emission coming from other dunes, whatever the atmospheric conditions. This gives rise to a second ill-posed problem: *what is the specific property of singing sands? Why do some sands sing and others not?* Most authors agree that singing sands are clean, rounded and polished [28, 29, 30, 71] and have a very narrow size distribution (figure 2). However,
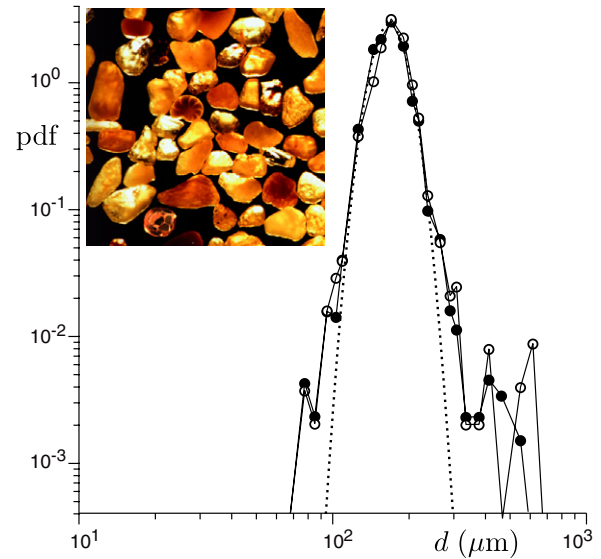

Figure 2. Grain size distribution of a singing sand sampled in the middle of the slip face of a mega-barchan (Sidi-Aghfinir, Atlantic Sahara) in 2001 (○) and 2009 (●). Technically, the graph shows the probability density function, weighted in mass, of the logarithm of the sand grain size d. The dotted line parabola is the best fit by a log-normal distribution, which allows one to define a mean grain size, $d = 167\,\mu$m within $1\,\mu$m of uncertainty, and the width of the distribution ($\simeq 0.1$). Inlet: microscope image of the grains.

all aeolian dunes are sieved by the wind and present such a distribution in the middle of their slip face.

It has been proposed that singing sands would present a silica gel layer at their surface [47]. However, this was inferred very indirectly from the presence of a broadband at $3400\,\text{cm}^{-1}$ in the infrared molecular vibration spectrum, a frequency which corresponds to the vibration of –OH bonds (but not exclusively). From this observation, Goldsack *et al* concluded that water is trapped at the surface of the grains, and from that, the presence of a silica gel coating [47]. They probably came to this questionable conclusion after they observed that silica gel itself emits sound when sheared in a jar [65].

Other studies suggest that singing sands would be covered by desert varnish, composed of glued silts and oxides, which would increase the microscopic friction between grains [33, 34, 93]. Applying this idea, different groups have successfully produced artificial singing sands from spherical glass beads [33, 77, 78, 80].

In this review, we will deny the relevance of the singing versus non-singing sand issue. First, the number of booming dunes does not have any profound meaning. In their pioneering work, Bolton and Julien have for instance identified more than 200 spots in the US [16–19]. The Atlantic Sahara region contains more than 10 000 booming dunes [42]. Three of them—large mega-barchans that behave like giant solar ovens—can emit sound 350 days per year as they are almost always dry on the surface; most of the smaller dunes can emit only a few tens of minutes per year, when the weather is sunny, very hot and not windy, so that the dry surface sand layer is sufficiently thick. Second, one of the most important results obtained in the last few years is the existence of a threshold avalanche thickness above which booming occurs (see below).
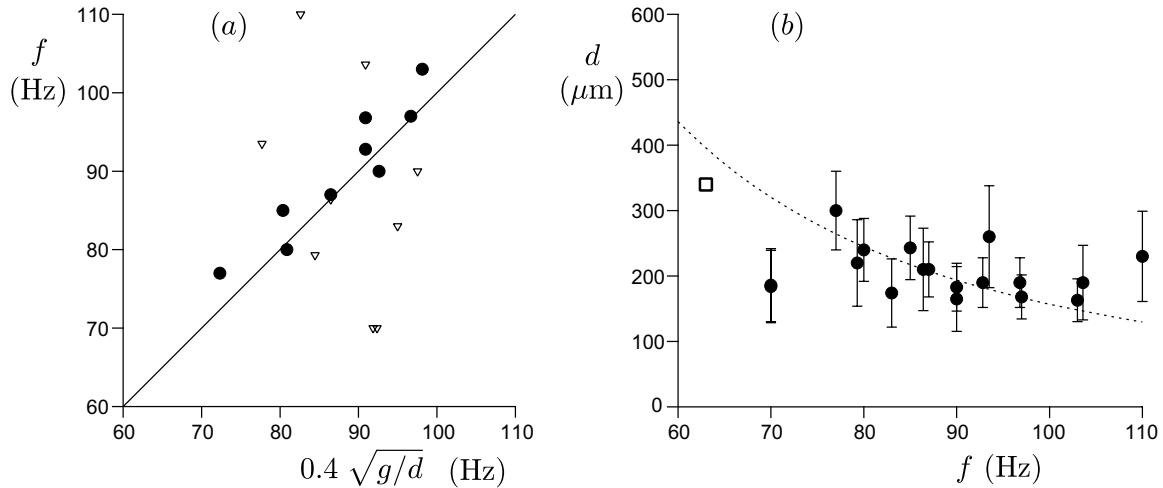
Figure 3. Emission frequency f of various booming dunes across the world as a function of the grain diameter d. Data from [33, 34, 56]. The very same data set is represented with two graphical conventions. (*a*) Fair choice of axes but emphasis on a fraction of the data set through the choice of symbols (after [6, 34]). (*b*) Stretched horizontal axis, compressed vertical axis and vertical error bars showing the width of the grain size distribution, rather than the error made on the measurement of the mean grain diameter (see figure 2) and of the mean emission frequency (after [56, 108, 107]). The lines correspond to the putative scaling law: $f \propto \sqrt{g/d}$.

Then, who could say if a sand dune reputed non-booming would emit sound if a 1 m thick avalanche could be generated. The correct formulation of the question could well be: *what are the characteristics of grains that lower the booming instability threshold?* The 'special' property would then be an intensity, and not a 'yes' or 'no' property.

Is the booming frequency set by the grain size? The third controversial question that cannot be scientifically settled is the dependence of the avalanche booming frequency f on the grain size d. From dimensional analysis based on gravity g, one can hypothesize that the frequency f scales as $\sqrt{g/d}$, which has the correct order of magnitude. As detailed in section 5.3, different emission mechanisms predict a frequency obeying this scaling law. Figure 3 shows two graphs obtained from the same booming dunes data set [34, 56] using two representations, one suggesting the validity of the scaling law [6, 34] and the other against it [56, 107, 108]. Figure 3(*a*) has a fair choice of axes but underlines the data points that fit the scaling relation by the choice of symbols; figure 3(*b*) squashes the data to visually suggest a lack of correlation. Our own conclusion is again that this question must be left aside as one can neither prove that it is correct nor prove that it is wrong. Let us detail the trap machinery. First, the definition of *the* grain size is problematic. Some use a grain size distribution weighted in mass and others weighted in grain number. Some use the fit of the grain size probability density function by a log-normal distribution (figure 2) or by a Gaussian while others measure the diameter d50 that separates the distribution into two parts of equal probability. Some carefully sample the sand at mid-height of the active slip face and others sample the dune and the surrounding zone. Therefore, the error bars for a given method can be relatively small but systematic effects can be huge. Second, one can talk about 'the' booming frequency only when avalanches are steady and homogeneous, and not pulsed by the slider. Otherwise, one gets a 'squeaking' emission due to the sand displaced with the body, superimposed on the 'booming' emission. Third, other properties of the grains

(surface roughness, friction, cohesion, capillary bridges) may quantitatively affect the frequency. We are not aware of a single controlled granular experiment where a scaling law with respect to the grain diameter has been verified with a precision better than 25%. Fourth, aeolian dunes are always composed of grains that can be entrained by the wind. The grain diameter d is thus never smaller than 150 μm, as the sand would be too cohesive, and never larger than 300 μm as the grains would be too heavy. Therefore, there is at best one octave of variation of the grain diameter. The emission frequency has itself a dynamics lower than one octave, as it ranges from 70 to 110 Hz depending on the location. On the one hand, no scaling law can seriously be inferred when the control parameter varies by less than an octave. On the other hand, the scaling law $f \propto \sqrt{g/d}$ is verified by all data points within error bars and cannot therefore be refuted. An objective look at the data only allows one to say that both the grain size and the emission frequency are fairly constant.

The present review will bypass these traps and focus on the following issues.

What are the objective characteristics of homogeneous steady booming avalanches? The main objective characteristics of booming sand avalanches will be reviewed: nature and localization of the source, frequency spectrum, frequency selection, coherence, amplitude, vibration modes and emission threshold.

What are the objective characteristics of shear induced emission? We will review the same properties for the various singing sand experiments performed in the laboratory, using controlled set-ups.

How does sound propagate in a sand dune? We will present the main properties of acoustics in granular media and detail the case of sand dunes.

What are the different emission mechanisms that have been proposed and how can/have they been tested? We will present and discuss the four main hypotheses: a passive resonance,

a stick-slip instability, a synchronization instability and an amplification of elastic waves by a sliding frictional interface.

2. Characteristics of booming sand avalanches

2.1. Sand vibration and emission in the air

Does the sound continue for several minutes, even after the avalanching of sand has ceased? The emission of sound in the air during a booming sand avalanche is associated with a vibration of the sand surface in the avalanche zone, but also in the surrounding region where there is no granular surface flow. The nature of the relation between the avalanche and the sound emission is the fourth controversy of the problem. Vriend, Hunt and co-workers at Caltech claim that booming lasts for minutes after the sand motion ceases [56, 107, 108]. If this were true, it would constitute a central piece of evidence that the phenomenon results from the passive resonance of the dune and not directly from the avalanche. However, no data have ever been published to support these statements [6]. Nothing is actually visible in the video presented in [107]; a possible explanation is that the sliders had this feeling, due to dynamically triggered avalanches flowing behind them.

Tests. It can be inferred from the orders of magnitude reported in [56, 107, 108] that this statement is implausible. One can estimate the Q factor of the dune resonator that would be needed to obtain a resonant emission during several minutes. The Q factor is the product of the angular frequency (typically $2\pi \times 100$ Hz) and the sound decay time (100 s according to [56, 107, 108]). This gives a Q factor slightly lower than 10^5, which is the Q factor of a quartz oscillator, not that of a sand pile. If this were true, then any noise, even an insect walking on the sand, would lead to a very loud resonant emission of the dune. This is not the case.

If sound emission after grains completely stop were real, it would be easy to prove it: one would just need to present objective movies of the whole slip face, with a synchronized sound record. Then, the time lag between the end of the avalanche and the end of the sound could be measured. We have ourselves performed such measurements over several hundred avalanches in the Atlantic Sahara. The sound systematically ceases *before* the sand stops moving, when the flow thickness has decreased below a threshold value. Unless a proof is produced, one can thus consider that the sound does not continue after the avalanching of sand has ceased.

The loud-speaker model. The surface of the sand bed acts as the membrane of a loud speaker and its vibration is directly responsible for the acoustic emission in the air [4]. As shown in figure 4, the surface normal acceleration is approximately in phase with the pressure time derivative. Laboratory experiments have confirmed that it is the same for a loud speaker whose membrane is covered by sand [4]. Furthermore, the power I emitted per unit surface in the air, measured with the microphone, is related to the mean square acceleration of the free surface $\langle a^2 \rangle$ by

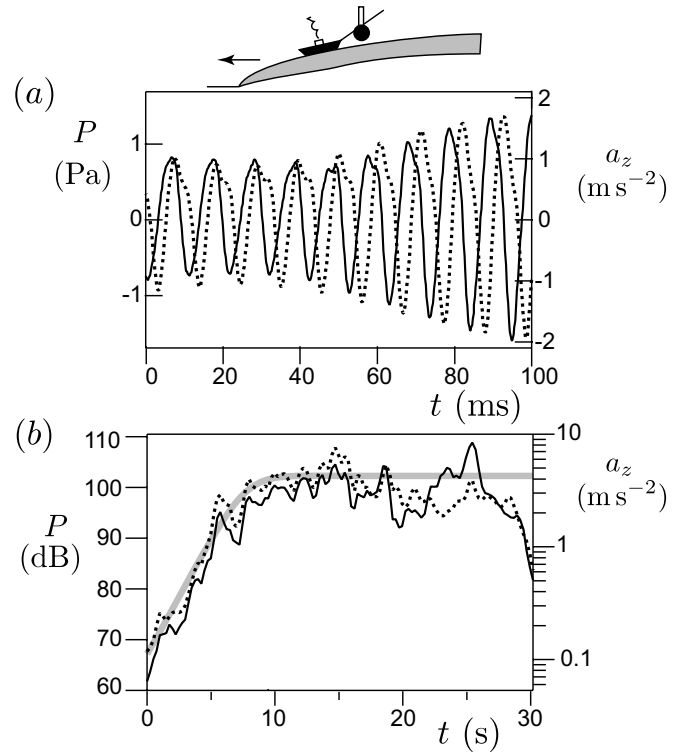$$I = \frac{\rho_{air} c_{air} \langle a^2 \rangle}{(2\pi f)^2} \qquad (1)$$

Figure 4. Simultaneous measurements of the acoustic pressure p in the air (dotted line) and of the normal acceleration a_z (solid line) at the free surface of a booming avalanche (Sidi-Aghfinir). The scales are chosen such that the signals have equal amplitudes, if the sand surface behaves like the membrane of a loud speaker. (*a*) Signal sample. Note the quadrature between pressure and acceleration, as predicted by the loud-speaker model. (*b*) Amplitude of the signals as functions of time t. The grey line is the best fit by equation (2), assuming that the avalanche propagates without changing shape. It underlines the exponential growth of the signal and its saturation. Measurements performed by Andreotti [4].

where ρ_{air} is the density of air and c_{air} the sound velocity in air. The sound is incredibly loud as the amplitude usually reaches 100 to 105 dB in the core of the avalanche.

2.2. Frequency

As revealed by the frequency spectrum (figure 5(*b*)), the song of dunes is not a noise but is a low-pitch sound with a well-defined central frequency f. When a good linear transducer, like a centimetre-scale accelerometer at the surface of the avalanche, is used to measure the signal, no strong harmonic content is observed. The amplitude of harmonics decays faster than algebraically with the order n—it usually decays exponentially with n for acceleration signals measured at the surface of booming avalanches (figure 5(*b*)). The sound emitted in the air is less noisy and presents harmonics of larger amplitudes than the acceleration signal, in particular above 100 dB [50, 71]. Harmonics are then associated with an asymmetry between downward and upward acceleration components. The possible effects leading to these harmonics include non-linearities of the emission mechanism, of acoustic propagation along the dune surface [35, 61, 62, 64, 102–104] and of intrusive transducers. Harmonics of higher amplitudes
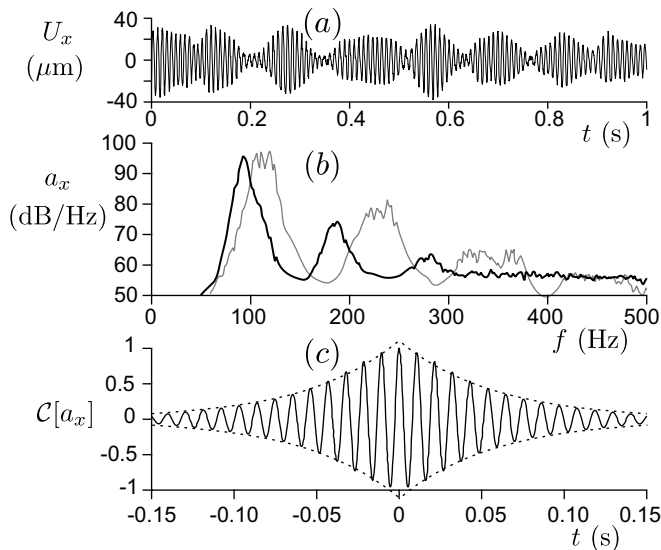
Figure 5. Spectral content of the song of dunes. (*a*) Signal of the displacement component U_x parallel to the surface. Note the amplitude modulation which points to the existence of very close frequencies in the signal (a doublet in the present case). (*b*) Power spectral density of the acceleration signal a_x. The normalization is chosen to give the acoustic power, according to the loud-speaker model. Note the exponential decay of the amplitude of harmonics with the order n. (*c*) Auto-correlation $\mathcal{C}[a_x]$ of the acceleration signal a_x. The fit of the envelope by an exponential (dotted line) gives the coherence time (which ranges from five to ten periods). The solid line in the three panels corresponds to a record in Sidi-Aghfinir (Atlantic Sahara). The grey line in panel (*b*) corresponds to a record in Al Ashkharah (J'alan) where the different modes composing the peak can be observed. Measurements performed by Andreotti and Bonneau [4, 7].

can be obtained by beating the legs to pulse the avalanche [56, 107]. Using the body fully to induce and modulate sand motion, the dune can even be played like a musical instrument. In the following, unless otherwise mentioned, the frequency f denotes the fundamental frequency measured when avalanches are induced in a steady homogeneous way.

The musical quality of the sound mostly results from a large tremolo (amplitude modulation) and a small vibrato (frequency modulation), which are effects known to induce emotions and a feeling of harmony (figure 5(*a*)). This modulation shows that the frequency peak observed in the spectrum is actually composed of a series of peaks (at least two) of neighbouring frequencies (grey line in figure 5(*b*)). While almost all spontaneous acoustic phenomena present harmonics, such a regular amplitude modulation is quite uncommon in nature.

2.3. Coherence

The existence of a well-defined frequency f immediately raises the question of frequency selection. It can be observed in figure 5(*b*) that the width of the frequency peak is typically 20 Hz. This can be seen even more clearly in the auto-correlation signal of figure 5(*c*), whose envelope decays exponentially over five periods. One can deduce the Q factor, which quantifies the frequency selection or equivalently the phase coherence and which ranges from 30 to 60.

We have already underlined the fact that the frequency f does not vary much from place to place and ranges from 70 to 110 Hz. At a given place, the range of variation of the frequency is even smaller. We have ourselves accumulated the largest data set (a few thousand minute-long records over eight years) of spontaneous (wind induced) and triggered (man induced) booming avalanches at the same place (Sidi-Aghfinir mega-barchan, Atlantic Sahara). Whatever the position of the avalanche on the dune slip face and whatever the weather conditions, the frequency determined by auto-correlation over the whole run was systematically between 92 and 107 Hz. Similar results were obtained on the large Dumont dune where the frequency of sustained booming was systematically between 77 and 92 Hz (seven records over four years [107]). As discussed in section 1.3, there is no point discussing such a narrow range of variation (15 Hz).

These observations allow us to formulate the physical problem posed by booming dunes through three questions. *What are the dynamical mechanisms responsible for the spontaneous acoustic emission? What picks up the rather well-selected emission frequency f? Why is the frequency peak composed of several neighbouring frequencies?*

2.4. Acoustic source localization

The acoustic emission in the air is directly due to the vibration of the sand free surface, which behaves like the membrane of a loud speaker and which is thus the source of the sound emitted in the air. The nature of the source of sand vibration has led to the fifth controversy of the subject. *Is the seismic source the avalanche or the dune?* In order to answer this question, we need to clarify the notion of source. From the energetic point of view, the source of acoustic energy is, without any doubt, the avalanche, since the rest of the dune is dissipative. From the signal point of view, we can define the acoustic source as the locus of the frequency selection.

Tests. With this definition, the dune would be the source if it were acting as a selective filter of a broadband noise emitted by the avalanche. This suggests two simple tests. *Is there a coherent vibration at frequency f inside the avalanche? Is the vibration amplitude at the frequency f larger outside the avalanche than inside?*

2.5. Amplitude

A vibration amplitude $\mathcal{A}$ can indifferently be measured from an acceleration, a pressure, a velocity or a displacement signal. Assuming that the avalanche is a travelling wave that propagates without changing shape [38], the measurement of the amplitude at a fixed point, as a function of time, allows one to determine the spatial profile $\mathcal{A}(x)$ in the moving frame of reference. On the booming dunes where such measurements have been performed, it has been systematically observed that the sand vibration amplitude is maximal inside the avalanche (figure 6(*a*)). Outside the avalanche, the vibration amplitude decays roughly as the inverse of the square root of the distance to the centre of the source. The dune thus behaves passively, as expected. This means, in particular, that the avalanche is *not* a source of noise but vibrates coherently at the frequency f.
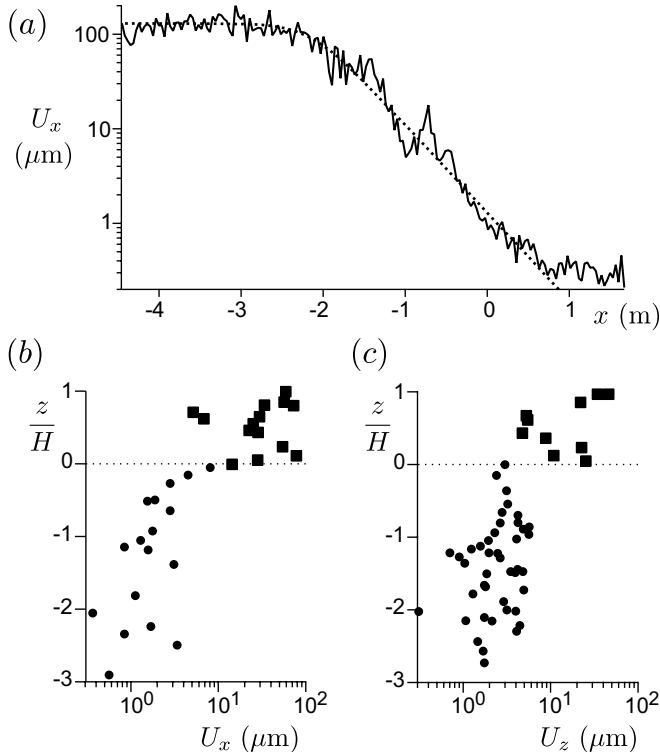
Figure 6. Spatial profiles of the vibration peak-to-peak amplitude. x is the axis along the steepest slope, parallel to the surface, and z the axis normal to the free surface. (*a*) Longitudinal profile of the displacement component U_x. The origin $x = 0$ corresponds to the avalanche front. The avalanche is located in the zone $x < 0$. The dotted line corresponds to the best fit by equation (2). It shows the exponential amplification of elastic waves and their saturation after a few metres. (*b*) Profile of the displacement component U_x along the normal axis z, normalized by the avalanche thickness H. $z/H = 1$ corresponds to the free surface and $z/H = 0$ to the interface between static and moving grains. (*c*) The same, but for the displacement component U_z. The vibration amplitude drops by a factor of ten across the interface separating the avalanche from the dune. Measurements performed by Andreotti and Bonneau [7].

The avalanche is thus the seismic source, i.e. the place where the frequency is selected.

Inside the avalanche, the vibration amplitude $\mathcal{A}$ increases exponentially from the front to the centre and saturates at a value $\mathcal{A}_\infty$ in the core of the avalanche. This growth has been interpreted in [7] as a signature of a dynamic amplification of elastic waves propagating up the slope. Assuming that booming results from a convective instability and using a symmetry argument, one can write a Ginzburg–Landau equation of the form

$$\partial_x \mathcal{A} = -q\,\mathcal{A}\left(1 - \frac{\mathcal{A}^2}{\mathcal{A}_\infty^2}\right) \qquad (2)$$

where x is the downslope space coordinate, in the frame of reference of the avalanche, and q is the space amplification. The $\mathcal{A}^3$ term encodes the effect of the first non-linearities. The solution of this equation takes the form

$$\mathcal{A} = \frac{\mathcal{A}_\infty}{\sqrt{1 + \eta \exp(2qx)}} \qquad (3)$$

where η is determined by the signal level at the front. Figures 4(*b*) and 6(*a*) show that it provides a reasonable fit to the data.

The longitudinal component of displacement U_x typically saturates to a peak-to-peak amplitude of $\simeq 80\,\mu$m (figure 6(*b*)) and the vertical component U_z to $\simeq 40\,\mu$m (figure 6(*c*)). The typical strain is thus around 10^{-3}, a value large enough to suggest the presence of non-linear effects in the acoustic propagation (see section 4). Using the loud-speaker model, the above values correspond to a sound amplitude around 105 dB, as measured using pressure transducers in the air. They also correspond to a peak normal acceleration (a_z) of $\simeq 8\,\mathrm{m\,s^{-2}}$. This value is usually found within a factor of two of the gravity acceleration g. It has thus been hypothesized that the vibration amplitude is limited by gravity [4]. Indeed, when a_z reaches $g\cos\theta$, where θ is the free surface angle, the grains on the surface must take off and form a gaseous granular layer.

These values correspond to the ideal situation where the sand is perfectly dry and the avalanche well developed. However, the vibration amplitude in the core of the avalanche depends on the experimental conditions. For instance, small amounts of atmospheric humidity, which creates capillary bridges between the grains, effectively preclude booming emissions in these desert sands [70]. The sound amplitude also depends on the length L of the avalanche: when the avalanche gets smaller and smaller, the vibration is less amplified so that the sound gets weaker and weaker. As argued in [39], there are even conditions under which booming is completely inhibited, which suggests the existence of a true instability threshold. As a matter of fact, the amplitude can nonetheless depend on humidity and on the avalanche length L but also on other parameters such as the flowing height H and the avalanche velocity V. As H, L and V are coupled, and related to the free surface slope, it is difficult to conclude on the nature of the relevant non-dimensional parameter controlling the emission threshold. A discussion of this parameter based on field measurements remains unsubstantiated. In the following, we will see that laboratory experiments allow us to investigate this issue in a deeper way.

2.6. Vibration modes

We have seen that, on the surface, the vibration is larger outside the core of the avalanche than inside. The hypothesis of a resonant mode of the dune raises the sixth controversy on booming dunes. *Does the dune vibrate in depth?* A series of acoustic measurements have been performed by Vriend *et al* [56, 107] using an array of geophones positioned *at the surface*. Once analysed in terms of *bulk* elastic waves (see section 4), they suggest that the dune, far from the avalanche, vibrates at several metres below the surface. On the other hand, dynamical mechanisms for which the avalanche is the source should lead to a vibration localized at the surface.

Tests. In order to test whether or not dune resonant modes are excited by the avalanche, it is necessary to measure the vibration below the sand surface, in depth, to locate a putative vibration antinode. The profiles of vibration amplitude measured normal to the free surface show that the vibration

mostly takes place inside the avalanche (figures 6(*b*) and (*c*)). Across the interface separating the avalanche from the static dune, the vibration amplitude drops by more than one order of magnitude. At 20 cm below the surface, the amplitude is two orders of magnitude lower than on the surface. Although these measurements need to be reproduced by other groups, one may already conclude that the vibration profile does not resemble the profile of a mode '$\lambda/4$' resonating over a metre scale surface layer.

2.7. Shear localization

It has been hypothesized by Patitsas [85, 86] that the formation of shear bands is necessary to get an acoustic emission. Indeed, booming avalanches typically have a centimetre-scale thickness. Looking at the surface of such an avalanche from above, one observes a coherent solid-like motion over blocks as large as a few tens of centimetres. This would be consistent with shear band localization. It is possible to obtain semi-quantitative information about the velocity profile by plunging metallic blades covered with black soot inside the avalanche [6]. Having in mind that the blade probably induces disturbances, analysis of the erosion of the soot reinforces the hypothesis of shear localization. We will see that laboratory experiments tend to confirm this idea.

3. Laboratory booming shear flows

Sonic sands emit sound when sheared at a sufficiently high rate in many different experimental situations. Whatever the geometry, booming granular flows form shear bands localized either in the bulk or along a boundary. These laboratory booming shear flows allow us to discuss more deeply four questions: the instability threshold, the velocity profile, the coupling between mean flow and vibration, and the relation between geometry of the pile and emission frequency.

3.1. Plow experiment

Instability threshold. Figure 7 shows the principle of the plow experiment, also called the bulldozer experiment. A plow (a solid plate for instance) is moved at a constant speed V inside a sand bed. It entrains a volume of sand into motion, characterized by its height H, its width W and its length L. These characteristics depend on the depth at which the plow is pushed in and on the geometry of the initial sand layer (flat, forming a crest or a trough). The plow can be rotated at a constant angular speed or moved in translation.

The structure of the flow is shown in figure 7(*a*). The free surface presents a slope slightly higher than the dynamic friction coefficient. The entrained mass has a velocity almost equal to that of the plow; looking at the granular flow in the frame of reference of the plow, one observes a residual vortical motion consistent with the slope. The moving grains are separated from the static sand bed by a shear band whose thickness scales on the grain diameter d. The shear rate $\dot{\gamma}$ thus scales as V/d. Figure 7(*a*) shows that $\dot{\gamma}$ is strongly heterogeneous and is maximal near the two 'contact lines', at

both ends of the shear band. For a sufficiently large entrained volume, the characteristics of the flow depend on a single parameter, the Froude number, which compares the dynamic pressure $\propto \rho_s V^2$ to the gravity induced pressure $\propto \rho_s g H$:

$$\mathcal{F} = \frac{V}{\sqrt{gH}}. \tag{4}$$

The controlled experiment performed by Douady *et al* [34, 39] was the first to highlight the existence of a threshold above which booming occurs. Typical results are shown in figure 7(*b*). They suggest that there are actually two thresholds: one controlled by the pile geometry and the other by a dynamical characteristic of the flow. First, booming can only occur when the height H is sufficiently large, for $H > H_{th}$. For a given H above this threshold value, a minimal Froude number $\mathcal{F}_{th}$ is needed (dotted line in figure 7(*b*)).

On this basis, we can reformulate the question of the 'specific' properties of singing sands. *What are the material parameters and the operating conditions that have an influence on the booming threshold?* As observed for booming avalanches in the field, it has been shown by Dagois-Bohy *et al* [34] that the ambient humidity increases the threshold in H and V (arrows in figure 7(*b*)). To give a quantitative idea, when going from 25% to 50% humidity, the threshold Froude number $\mathcal{F}_{th}$ rises from 0.5 to 0.8 and the threshold height H_{th} from 3 to 5 cm.

The second key parameter controlling the acoustic properties of singing sand is the microscopic friction between grains, $\mu_\mu = \tan(\theta_\mu)$ [28–30]. Indeed, according to Dagois-Bohy *et al*, most singing sand grains are coated with a desert varnish composed of silicate-iron and manganese oxides along with silts [33]. This varnish leads to a microscopic friction angle $\theta_\mu \simeq 20°$ twice larger than that of glass beads ($\theta_\mu \simeq 10°$). When the glass beads are artificially coated with silt and clay extracted from natural singing sand, they become able to emit sound when sheared [34, 77, 78, 80]. Note that the microscopic friction must not be confused with the dynamic friction angle θ_d. The difference between the two $\theta_d - \theta_\mu \simeq 13°$ results from a geometrical effect [3].

Frequency selection. Figure 7(*c*) shows three sets of frequency measurements performed with the same rotating plow set-up, for different shapes of the sand bed. Contrary to gravity-driven avalanches on dunes, the frequency f varies over two octaves, when the plow velocity V and the depth at which it is dug into the sand bed are changed. For given operating conditions, the relation between the emission frequency f and the ratio V/H is well approximated by an affine function of the form

$$f = f_0 + \alpha \frac{V}{H} \tag{5}$$

where f_0 is around the emission frequency measured in the field, for gravity controlled avalanches and α is a multiplicative constant. The interpretation of this curve constitutes the seventh controversy of the problem. It has been hypothesized by Poynting [90, 91] and followers [4, 6, 33, 39] that the frequency f corresponds to the shear rate $\dot{\gamma}$ inside the granular shear band. As the velocity of the grains on the surface
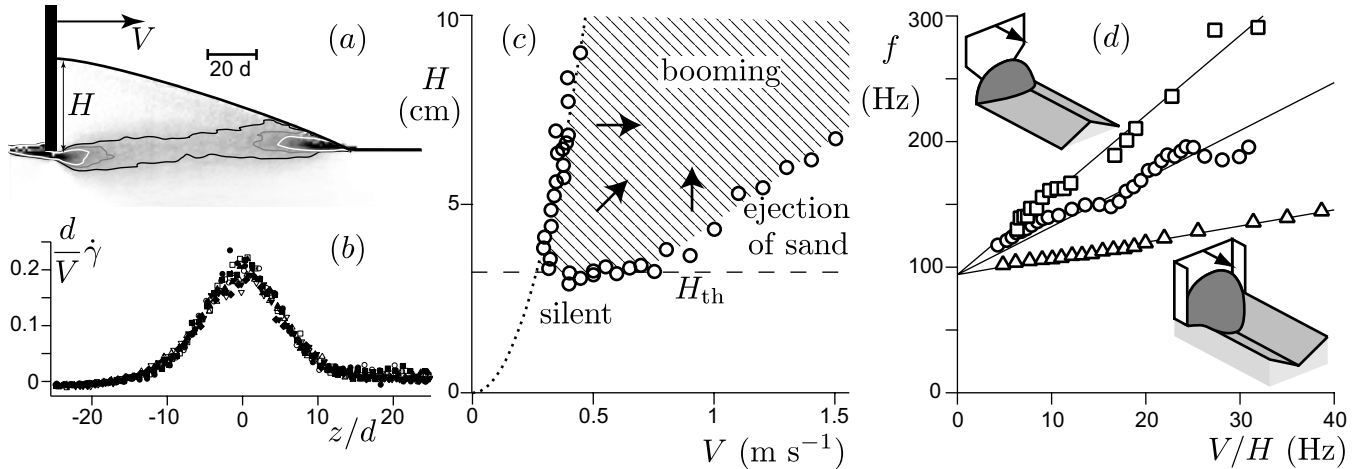
Figure 7. Plow experiment: a plate, dug into the sand, is pushed along the sand free surface at a constant speed. (*a*) Numerical simulation of the experiment using a discrete element method. Greyscale shows the shear rate $\dot{\gamma}$. Isocontours correspond to $d\dot{\gamma}/V = 0.1$ (black), 0.15 (grey) and 0.2 (white). The flow presents a shear localization over a few grain diameters, with a stress amplification close to the two geometrical singularities. Simulations from Percier *et al* [87]. (*b*) Profile of the rescaled shear rate $d\dot{\gamma}/V$, measured in the middle of the flowing region (see (*a*)), for a series of simulations at different H, for $V = 5\sqrt{gd}$. (*c*) Parameter range for sound emission (shaded area), depending on the plow velocity V and the height of pushed sand H. Booming occurs above a threshold height H_{th} (dashed line: $H_{th} \simeq 3$ cm) and a threshold Froude number $\mathcal{F}_{th}$ (dotted line: $\mathcal{F}_{th} \simeq 0.5$). At very large velocities, the grains entrained by the plow are ejected and the acoustic emission stops. The black arrows illustrate the displacement of the threshold when humidity increases. (*d*) Emission frequency f as a function of the ratio H/V for different initial shapes of the sand layer: starting from a crest for □ (measurements performed at the booming threshold by Douady *et al* [39]) and ○ (measurements performed at a low humidity of 25% by Dagois-Bohy [34]) or from a trough for △ (measurements performed by the author). The solid lines show the best fit by the form $f = f_0 + \alpha V/H$, where $f_0 = 94$ Hz is the booming frequency measured in the field. The slopes are, respectively, $\alpha = 1.3$ (△), 3.8 (○) and 6.4 (□). When possible, measurements are averaged over ten data points.

is close to the plow velocity V, the average shear rate over the flowing region is $\simeq V/H$. Douady *et al* have therefore interpreted equation (5) as direct experimental evidence of the equality $f = \dot{\gamma}$. However, several facts are in conflict with this working hypothesis. First, equation (5) is not a relation of proportionality between f and V/H: f_0 is far from negligible. Second, the slope α is not 1 and varies by a factor of five when the experiment is started from a sand bed with a crest (□ in figure 7(*d*)) or with a trough (△ in figure 7(*d*)). Third, the plow experiment presents shear localization over a band width set by the grain diameter d, which leads to the scaling law $\dot{\gamma} \propto V/d$ (figure 7*b*)) and not $\dot{\gamma} \propto V/H$. Fourth, the field of $\dot{\gamma}$ is not homogeneous; across the shear band, $\dot{\gamma}$ typically presents a Gaussian profile.

In conclusion, we can formalize two more questions on singing sands. *If the frequency is not controlled by the flow velocity field, why does it depend on the plow velocity V? What is the velocity field inside a booming sand flow?* To answer the first of these questions, let us consider the problem of the drag force exerted by the sand grains on the plow. Just like the emission frequency, this force depends on the plow velocity V, which would suggest that a visco-plastic rheology governs the flow. However, when the drag force is plotted against the mass of grains entrained into motion, a simple linear relationship, which corresponds to a simple Coulomb friction, is obtained. This apparent contradiction results from the fact that the geometry of the flow is a function of the plow velocity V. In particular, for a given plow depth, the height H and the length L of the moving pile increase with V. Figure 8 shows the results obtained with a plow experiment performed in the field. It shows that the dependence of the frequency f
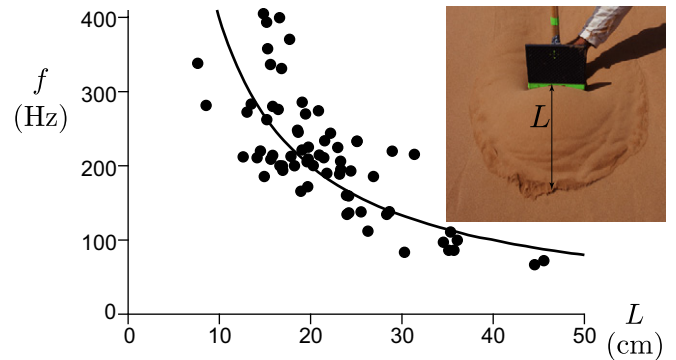

Figure 8. Plow experiment performed in the field with a rectangular plate, along the avalanche slip face (photograph in the inset). Relation between the booming frequency f and the length L of the avalanche, varying both V and H. The best fit by a relation of the form $f = \mathcal{C}/L$ (dotted line) gives a value $\mathcal{C} \simeq 40$ m s^{-1} close to the speed of sound under these conditions. Measurements performed by Andreotti and Bonneau for this review.

on V and H can be encoded into a dependence on the length L. Although scattered, data suggest a relation of the form $f \propto L^{-1}$, with a multiplicative factor close to the speed of sound in the granular medium (see section 4). As a conclusion, the frequency dependence in this type of plow experiment can be equally well represented by a kinematic quantity V/H or by the pile geometry.

Tests. In order to test whether or not the booming frequency f is related to the shear rate $\dot{\gamma}$, it is necessary to measure both quantities simultaneously, in the very same experiment. Moreover, to discriminate between the effects
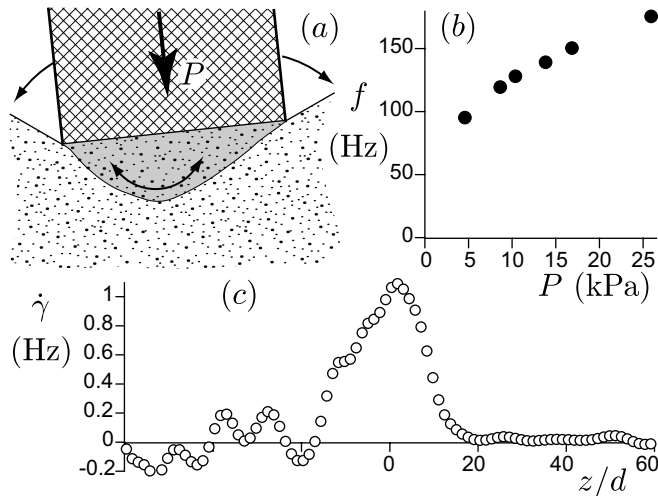
Figure 9. Rotating pestle experiment. (*a*) Experimental set-up: a solid block is rotated at the surface of a container full of sonic sand, under a controlled normal stress P. It entrains a lens of sand (grey zone) into rotation. (*b*) Relation between the emission frequency f and the normal stress P for a cylinder of diameter 85 mm and of mass $m = 2.65$ kg, using sonic sand from Sidi-Aghfinir. (*c*) Typical profile of the shear rate $\dot{\gamma}$ across the shear band. The emission frequency $f \simeq 100$ Hz, measured simultaneously, is much larger than $\dot{\gamma}$.

of geometry and shear, one should design an experiment where the shear band encloses a fixed geometry, whatever the velocity V.

3.2. Rotating pestle experiment

The simplest method to measure a velocity profile in a granular flow is to use a transparent glass boundary [4, 44]. However, confinement tends to suppress sound emission; moreover, the friction on this boundary is a dominant force which can control the whole flow [63]. To prepare this review, we have thus performed a plow experiment in which one can simultaneously measure (and vary) f and $\dot{\gamma}$. The set-up consists of a solid block rotating at the surface of a sonic sand and subjected to a constant vertical force (figure 9(*a*)). The flow is visualized through the lateral boundary but the cell is chosen sufficiently large to allow for the acoustic emission. As in the plow experiment, shear is localized in a shear band which separates a static region from a rotating one (figure 9(*c*)). This set-up presents the advantage of uncoupling the geometry, which remains almost invariant, from the shear rate $\dot{\gamma}$, which is proportional to the plow angular velocity. Our measurements show that the emission frequency f does not depend on $\dot{\gamma}$. For the example shown in figure 9(*c*), the frequency is ten times larger than f. For a given geometry (size of the pestle and of the container), f is completely controlled by the normal stress P and increases with it (figure 9(*b*)). Contrary to the impacting pestle experiment described next, the mass m of the pestle is not changed. The effect of P is, on the one hand, to change the stress distribution, and on the other hand to increase the speed of sound. Experimental data suggest that the emission frequency f corresponds to an acoustic mode (dependence on
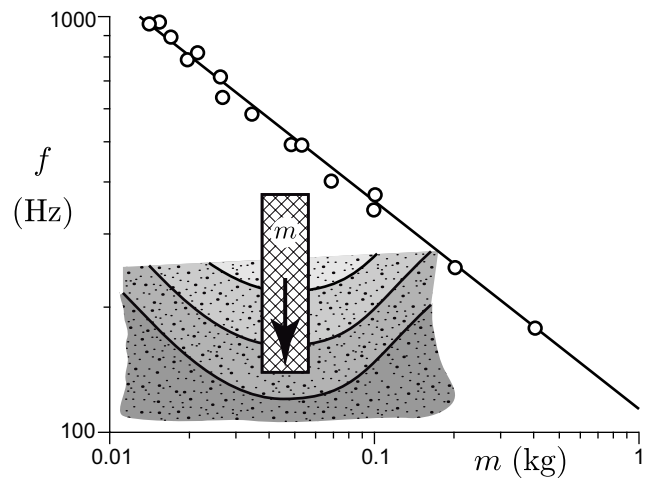

Figure 10. Frequency f of emission of a beach squeaking sand placed in a container and struck with a rod of mass m. Measurements performed by Nishiyama and Mori [80]. The solid line is the best fit by a power law: f follows a scaling law of the form $f \propto m^{-1/2}$ when the container is heavy enough not to vibrate. Inset: schematic of the experiment, after x-ray radiographs performed by [77]. Greyscale encodes volume fraction. The solid lines correspond to shear bands.

P in figure 9) selected by the geometry (dependence on L in figure 8).

3.3. Impacting pestle experiment

The action of the foot on a squeaking beach [96] can be abstracted into the impact of any heavy solid object in sand [100]. Figure 10 shows the results of the controlled experiment performed by Nishiyama and Mori [80]: a cylindrical pestle of mass m impacts sonic sand at a high constant velocity. In this geometry, the formation of shear bands was directly observed using x-ray radiographs by Miwa and collaborators [77] (see the inset of figure 10). Figure 10 shows that the frequency f scales as $m^{-1/2}$ over one decade. This suggests that f is in that case related to the natural frequency of the harmonic oscillator constituted by the sand (spring) and the pestle (mass). Nishiyama and Mori confirmed this hypothesis by directly measuring the spring constant k of their system and by comparing it with $m \ (2\pi f)^2$. This spring constant is much lower than that given by the elasticity of the solid pestle and of the container; estimates made using the results of section 4 show that k rather results from the elasticity of sand grains. In conclusion, the frequency emitted in the impacting pestle experiment—and thus on a squeaking beach—is related, as for the two previous experiments, to the elasticity of the granular packing. Moreover, this squeaking emission is obtained specifically when shear banding occurs [77]. Shear bands must thus play a role. Finally, in the impacting pestle experiment, the frequency f is determined by the inertia of the pestle and not that of the sand. This turns out to be an important difference between booming avalanches and squeaking beaches, explaining the high emission frequency in the latter case [96].
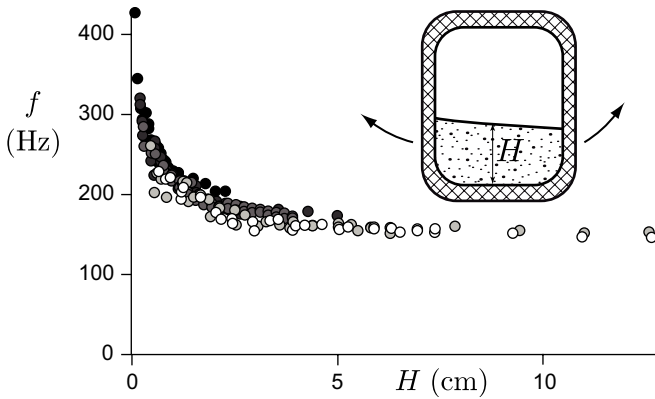
Figure 11. Frequency f emitted by sonic sand placed in a glass jar and shaked as a function of the sand thickness H. The grey level of symbols encodes the grain size, which ranges from $d = 197\,\mu m$ (white) to $d = 377\,\mu m$ (black). Measurements performed by Kilkenny [65, 67].

3.4. Jar experiment

In a different type of experiment (figure 11), granular matter flows along a boundary, and not perpendicularly as previously [52]. The easiest experiment consists in filling a glass jar with sonic sand and shaking it [50, 70]. Figure 11 shows a reinterpretation of the results obtained by Goldsack and collaborators [47, 67]. Although these authors concluded that the frequency was decreasing with the inverse of the grain diameter d, their results show otherwise: the curves obtained for different size fractions of the same booming sand collapse on a master curve, when plotted as a function of the sand thickness and not as a function of the number of sand grains in the jar. As in the previous experiments, the emission frequency f is a decreasing function of the sample size. More precisely, figure 11 shows that the frequency decreases rapidly with the flow thickness H at low H and tends to a constant at large H. The frequency is therefore selected by the granular packing geometry. Further experiments are needed to conclude precisely on the dependence of f with the jar radius.

It has been reported by Haff [50] that mixing five drops of water into a 1 litre bag full of booming sand can silence the acoustic emissions. As in the previous experiments, there is thus an instability threshold which depends on humidity.

3.5. Sand organ experiment

Experiment. During the discharge of a smooth elongated silo filled with granular matter (figure 12(a)), a loud sound is generally emitted [37, 79, 110]. This situation constitutes the archetype of flows for which a shear band forms along a rigid boundary. Contrary to the experiments previously described, the sand organ experiment does not require specific grains and can work with spherical glass beads. A necessary condition is lower friction between the grains and the boundary than between the grains themselves. Moreover, the booming amplitude increases with the grain roughness, just as in the song of dunes.

The mean flow velocity u_0 is controlled by the diameter of the outlet at the bottom end of the tube [14]. Thanks

to the wall friction, the pressure and density fields are homogeneous, except in the vicinity of the outlet and of the free surface [13, 84]. Just above the outlet, the signals are essentially low-amplitude noises characterized by a broadband spectrum. At a few tube diameters above the outlet, one observes the emergence of elastic waves at a well-defined frequency f (figure 12(c)) which is constant over the whole tube. f is independent of the length of the silo, so that the hypothesis of resonant standing modes can be rejected. The emitted frequency f does not depend strongly on the flow rate or on the tube radius and ranges from 60 to 90 Hz (figure 12(d)).

It has been shown experimentally by Bonneau et al [22] that spontaneous acoustic emission results from a linear convective instability [54]:

- the vibration results from elastic waves propagating exclusively up the tube.
- the vibration amplitude $\mathcal{A}$ increases exponentially from the outlet towards the top of the tube and saturates at a value $\mathcal{A}_\infty$, on the order of the gravity acceleration constant g. This amplification, shown in figure 12(b), is well fitted by equation (3), which is the solution of the Ginzburg–Landau equation (2).
- the dependence of the frequency f on the tube radius R and the flow velocity u_0 is very weak (figure 12(d)).
- the wavelength λ is selected by the tube radius R (figure 12(e)).
- the spatial growth rate $q(f)$ of the mode of frequency f is positive in a frequency band and presents a maximum that corresponds to the spontaneous emission frequency f (figure 12(c)). This means that random fluctuations around the outlet are selectively amplified around f during wave propagation.

A simple model. As the emitted wavelength is much larger than the tube radius, the system can be thought of as a 1D compressible system (the Janssen approximation [59]). Introducing the density ρ, the velocity u and the total axial stress $P + p$, averaged over the section of the tube (figure 12(a)), the continuity and momentum equations can be written in the form

$$\dot{\rho} + \rho \partial_z u = 0$$

and

$$\rho a = \rho \dot{u} = \rho g - \partial_z (P + p) - 2\mu (P + p)/R \qquad (6)$$

where μ is the grain-tube friction coefficient. Due to the mean flow u_0, the local velocity is always downwards so that the wall friction force is oriented upwards. On average, the grain weight is balanced by this friction. At equilibrium, in a long tube, the axial stress is thus a constant controlled by the tube radius: $P = \rho g R/(2\mu)$. We introduce the speed of compression waves c and the bulk kinematic viscosity ν. We denote by $\tilde{\rho}$, $\tilde{u}$ and p the disturbances of density, velocity and axial stress associated with the waves. In the reference frame of the moving sand, the continuity equation, the dynamical equation and the constitutive relation are linearized into

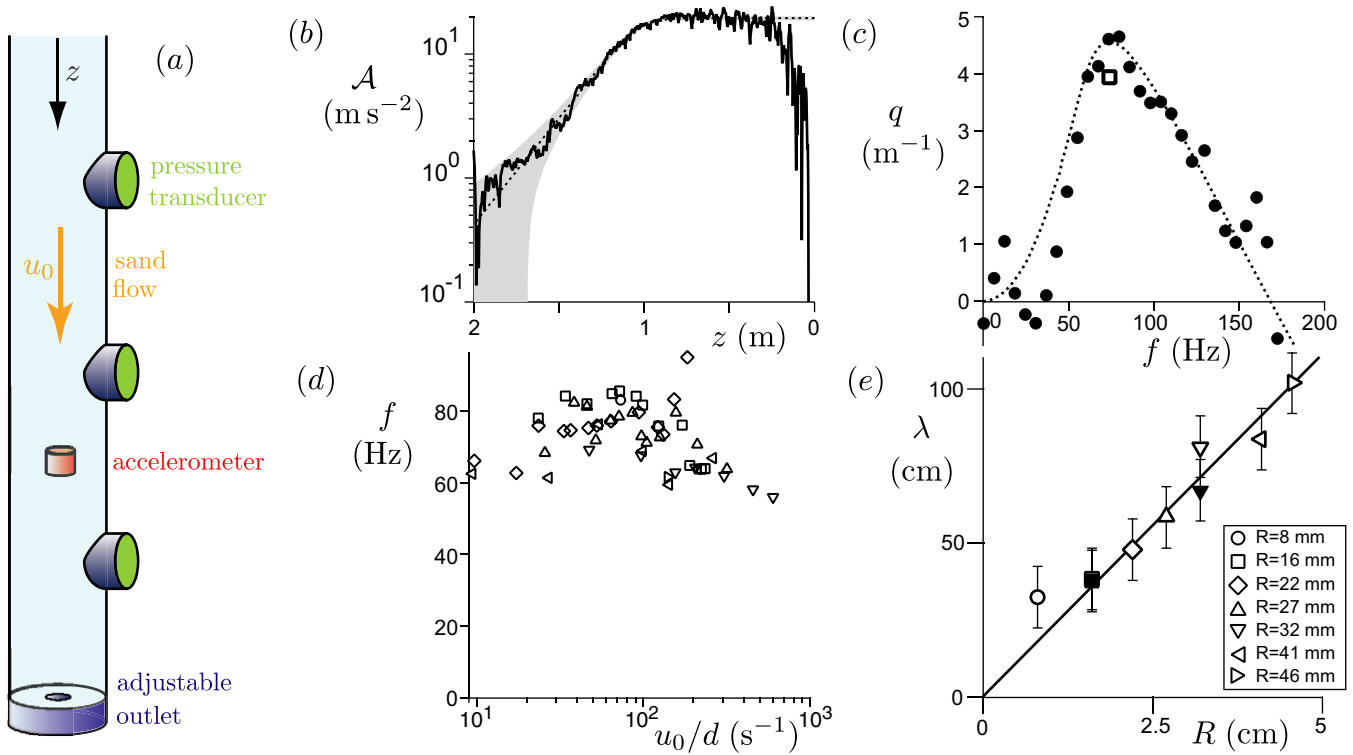$$\partial_t \tilde{\rho} = -\rho \partial_z \tilde{u} \qquad (7)$$

Figure 12. Sand organ experiment. (*a*) Experimental set-up. Gravity-driven granular flows are generated inside 2 m long tubes of radius R, ranging from 10 mm to 100 mm. In order to control the mean flow velocity u_0, the bottom end of the tube is fitted by a PVC plug in which a cylindrical outlet is reamed. The hole diameter is varied from $20d$ to $1.5R$. (*b*) Amplitude $\mathcal{A}$ of the acceleration signal as a function of the vertical coordinate z. The dotted line shows the best fit by the amplitude equation (3). (*c*) Spatial growth rate q as a function of frequency f (●). The square shows the value of q determined from (*b*). The emission frequency $f \simeq 75$ Hz coincides with the maximum of the growth rate. (*d*) Measured frequency f as a function of u_0/d. (*e*) Measured wavelength λ as a function of the tube radius R, for $u_0/d = 100 \pm 20\,\text{s}^{-1}$; black: $d = 165\,\mu$m; white: $d = 325\,\mu$m.

$$\rho \partial_t \tilde{u} = \tilde{\rho} g - \partial_z p - \frac{2\mu}{R} p \qquad (8)$$

$$p = c^2 \tilde{\rho} + \nu \partial_t \tilde{\rho}. \qquad (9)$$

As the steady state is homogeneous in space and time, the solutions of the linearized equations are superpositions of Fourier modes of the form $\exp(\mathrm{j}(\omega t + kz))$, where both ω and k can *a priori* be complex. The dispersion relation takes the form

$$\frac{\omega^2}{c^2 + \mathrm{i}\nu\omega} = k^2 - \mathrm{j}\frac{2}{\ell} k \qquad (10)$$

where the length ℓ is given by

$$\ell = \left(\frac{\mu}{R} - \frac{g}{2c^2}\right)^{-1} \simeq \frac{R}{\mu}.$$

In the limit of infinite ℓ and vanishing ν, one recovers the standard Helmoltz equation: acoustic waves can propagate in both directions at the velocity c. The viscosity ν damps high-frequency waves.

The unusual term in ℓ^{-1} is due to friction; it is non-conservative and operates in quadrature with respect to the restoring force. Importantly, it breaks the symmetry between upward and downward propagation, due to the polarization of the friction force. When one emits a wave in a static silo, the friction is everywhere opposed to the velocity of the grains at the boundary. The wave is thus attenuated. If one adds a mean

downward velocity, friction remains orientated upwards and becomes a source of acoustic amplification.

The frictional term in ℓ^{-1} is responsible for the convective instability: the dispersion relation (10) predicts the existence of unstable modes that all propagate upwards in the tube. Figure 12(*c*) shows that the space growth rate $q = \mathcal{I}m(k)$ presents a maximum with respect to the frequency f, as observed. The quality factor $\mathcal{Q} = c\ell/\nu$ compares the amplification of waves by friction and their damping by viscosity. At large quality factors, the most amplified mode does not depend on ν and scales as

$$q = \frac{1}{\ell}, \qquad \mathcal{R}e(k) = \frac{1}{\sqrt{2}\,\ell}, \qquad 2\pi f = \sqrt{\frac{3}{2}}\frac{c}{\ell}. \qquad (11)$$

This predicts that the acoustic wavelength λ is proportional to the tube radius R, as observed experimentally (figure 12(*e*)). The frequency selected f is expected to scale as the ratio of c to R. Experimentally, it turns out that c increases roughly with $R^{1/2}$, which explains the small dependence of the frequency f with R (figure 12(*d*)). As detailed in the following section, one would rather expect a scaling of c as $R^{1/6}$, following equation (14).

The sand organ experiment shares striking similarities with natural booming avalanches: the frequency is insensitive to the working conditions and is between 60 and 100 Hz, the elastic wave amplitude is amplified exponentially in space, and

friction enhances the phenomenon. We will show in the last section that they may share the same dynamical mechanism responsible for spontaneous acoustic emission.

4. Sound propagation in sand dunes

In this section, we present the most prominent characteristics of acoustic propagation in weakly compressed granular media. The interested reader may find in [104] a more complete review of recent results in this field.

4.1. Consequences of heterogeneity for sound propagation in granular media

Compared with a standard elastic solid, granular media possess several original characteristics: they are heterogeneous, disordered and non-linear. Still, some of the vibration modes strongly resemble those observed in a continuous elastic medium and have a low dependence on the details of the granular arrangement. For this reason, they are related to the response of the effective medium constituted by the macroscopic granular assembly. Many other vibration modes are localized in space—for instance, a few grains forming an oscillating vortex in the bulk of the sample (figure 13(b)). They reflect the local disordered structure of the packing [72, 73, 99]. A consequence of this heterogeneity is that when a short sound pulse is emitted in a granular medium under controlled pressure, the received signal has two parts (figure 13(a)): a coherent part related to the effective medium, independent of the details of the pile, followed by a coda (speckle) due to multiple scattering of the signal in the sample [60]. The respective amplitude of the coherent signal and the coda strongly increases with the static pressure P and with the typical excitation frequency f [103]. In particular, strong scattering occurs when the wavelength becomes comparable to the grain size d. However, this condition is not restrictive, as a granular pile prepared without particular caution presents in general heterogeneities of volume fraction and of microstructure (distribution of contacts and of interparticular forces) on scales much larger than d.

The heterogeneity of the material has an important consequence for the choice of acoustic sensors. The vibration of a transducer—and therefore its signal—can be decomposed as a sum over acoustic modes. A particular mode contributes to this signal proportionally to its amplitude and to the modal projection of the transducer shape—or more precisely, the modal decomposition of the granular displacement field imposed by the transducer. A transducer of size close to the grain diameter d is mostly sensitive to acoustic modes localized in its vicinity. Conversely, to isolate the mean field coherent signal there must be a length-scale hierarchy between the grain size, the transducer size and finally, the acoustic wavelength.

4.2. Speed of sound

Like an ordinary elastic solid, the speed of sound (i.e. the propagation speed of the coherent signal) can be derived from
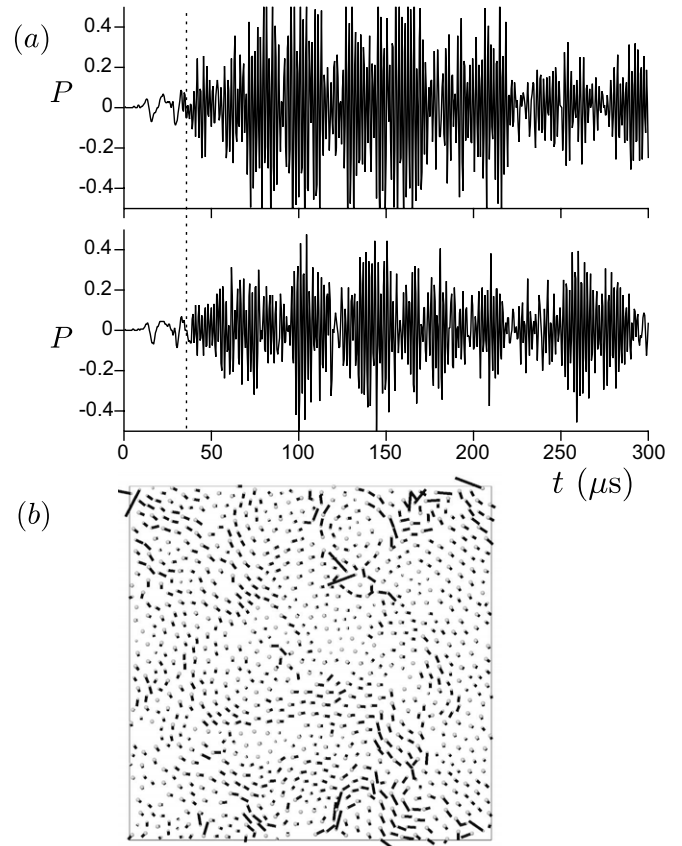

Figure 13. (a) Two examples of ultrasonic signals (broadband signal centred on 500 kHz) transmitted through a granular sample under high pressure ($P = 0.75$ MPa) for two different microscopic preparations. The coherent response of the effective medium is the fastest ($c \simeq 1000$ m s^{-1}) and is reproducible (left of the dotted line). This corresponds to an average wavelength of about 2 mm or equivalently 5 grain diameters. It is followed by a coda that corresponds to the signals propagating through all the heterogeneous paths of the system (right of the dotted line). This noise is the acoustic counterpart of optical speckle. Measurements performed by Jia *et al* [60]. (b) Example of a non-Fourier mode in a 2D granular system.

the elastic moduli K and G: $c \sim \sqrt{K/\rho}$ for compression waves and $c \sim \sqrt{G/\rho}$ for shear waves. Consider a large volume of grains at rest subjected to a confining pressure P. Let us follow a mean field approach where the strain field is assumed to be affine [20, 27, 41]. Then, by hypotheses, the forces are equally distributed between each contact between grains. The force on a contact then depends only on the particle relative displacement δ, through Hertz's contact law [3, 66].

As the pressure results from the sum of the contact forces divided by the surface of a grain, it is proportional to the average number of contacts per grain Z. The scaling law between the pressure P, the relative displacement δ and the average coordinance Z reads

$$P \sim \frac{ZF}{d^2} \sim ZE \left(\frac{\delta}{d}\right)^{3/2} \sim ZE\Delta^{3/2}, \qquad (12)$$

where $\Delta = -(\delta V / V)$ represents the relative variation of the volume occupied by the medium. The relative variation of distances is therefore $\Delta/3$. Let us consider this compressed
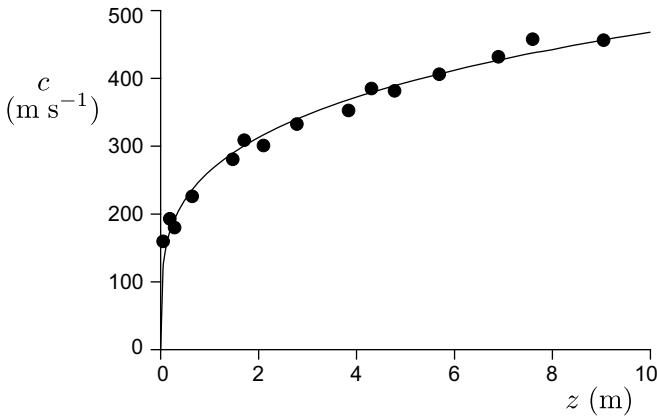
Figure 14. Dependence of the speed of sound c with depth z, measured on a booming dune by Vriend *et al* [107] by refraction of elastic waves. The best fit by a power law (solid line) gives an exponent around 1/4.

state as a base state to which a small perturbation in stress is applied. One obtains the scaling law followed by the bulk modulus [72]

$$K = -V\frac{\partial P}{\partial V} = \frac{\partial P}{\partial \Delta} \sim ZE(\Delta)^{1/2} \sim (ZE)^{2/3}P^{1/3}. \quad (13)$$

The mean field calculation predicts that the scaling law followed by the shear modulus G is the same as that followed by K [45, 83, 109]. From these expressions, one deduces the scaling law for the speed of sound [26]:

$$c \simeq \rho^{-1/2}(ZE)^{1/3}P^{1/6}, \quad (14)$$

where Z is the contact number, which also increases with pressure. The effective exponent of the power law relating c to P is around 1/4 (figure 14). As the speed of sound depends strongly on pressure, which is the physical signal that propagates, non-linear effects are exacerbated by granular media: dependence of sound propagation speed on the amplitude, generation of harmonics and subharmonics, existence of solitary waves, etc [35, 61, 62, 64, 102–104].

To highlight the meaning of relationship (14), it is sufficient to compare the speed of sound in bulk quartz ($\simeq 5000\,\mathrm{m\,s^{-1}}$) and in quartz grains at 10 cm below the bed surface ($\simeq 100\,\mathrm{m\,s^{-1}}$). c can become lower than the speed of sound in air, which points to the fact that a sand pile is amazingly soft. This impressive reduction of the speed of sound results from a simple geometric effect at the contact between grains: the area of contact depends on the normal load. In particular, the stiffness of two spheres brought into contact without normal force vanishes. As noted by Poynting [90], the resonant frequency of a single grain is larger than 10 MHz, which is much larger than booming frequencies f. By contrast, due to the geometrical effect, the resonant frequency of a sand layer of 5 cm is on the order of 200 Hz, which is the right order of magnitude.

4.3. Acoustic damping

Damping of acoustic waves in granular media may proceed from different dynamical mechanisms. Since granular media

are disordered, elastic waves are scattered by hetereogeneities present at all spatial scales. At small frequencies (below, say, 10 kHz), the acoustic wavelength is large compared with the grain size, so that the amplitude decays spatially as predicted by Rayleigh scattering. The attenuation is even larger at high frequencies, in the strong scattering regime (responsible for the coda tail in figure 13). Dissipation—transformation of mechanical energy into heat—is mostly localized in the region of contact between grains. It can result from solid friction between the surfaces in contact, which is itself ultimately related to the plasticity of micro-contacts [11].

The formation of capillary bridges between grains increases the dissipation of energy by linear viscous losses inside the water. The most dissipative zone is probably inside the grain contact area. Using common estimates for micro-contact geometry, the relaxation time in the presence of water should be on the order of $\simeq 1$ ms, which is consistent with the measurements performed at high frequency in [24]. This is two orders of magnitude smaller than the relaxation time measured for a dry sand layer. A secondary effect of capillary bridges is to increase the normal force exerted on grains: a capillary pressure, proportional to surface tension and to the inverse of the grain size, has to be added to the external pressure P.

Experiments performed in narrow tubes have shown that interstitial air can be a major source of acoustic dissipation [12]. The coupling between the elastic skeleton of the granular material and air surrounding grains can be understood using Biot theory of poroelasticity [1]. In the absence of coupling, three types of acoustic modes would exist: longitudinal and transverse modes in the solid and compressional waves in air. Due to its low acoustic impedance, compared with sand (4×10^2 versus $10^5\,\mathrm{Pa\,s\,m^{-1}}$), air does not have a strong influence on the modes associated with the propagation in the solid: air is entrained in phase with the grains and mostly causes viscous dissipation. By contrast, the mode associated with air, called a Biot wave, is strongly affected: due to the inertia of grains, the speed of this wave is much slower than the sound speed in air. Biot wave propagation is very dispersive and, since air and grains move in opposite phases, highly attenuated [1].

4.4. Modes guided by gravity induced index gradient

The pressure dependence of the speed of sound has a major consequence: in order to consider that the pressure P inside a sample is homogeneous, it must be at least 10 to 100 times larger than the pressure variation induced by gravity (ρgz, which is on the order of kPa). *How does sound propagate in sand under gravity?* The vertical pressure gradient induces an intense gradient in the speed of sound in the medium (figure 14). Like how waves arrive parallel to the beach regardless of their orientation away from the coast, acoustic wavefronts are deflected towards the free surface by a mirage effect: as the propagation is faster in depth than at the surface, the wavefronts rotate (figure 15). At the surface, the acoustic wave undergoes a total reflection, propagates back in depth, and so on. As in a gradient-index optical fibre, the propagation is therefore guided at the surface. For a given wavelength λ, propagation takes place through a discrete number of guided
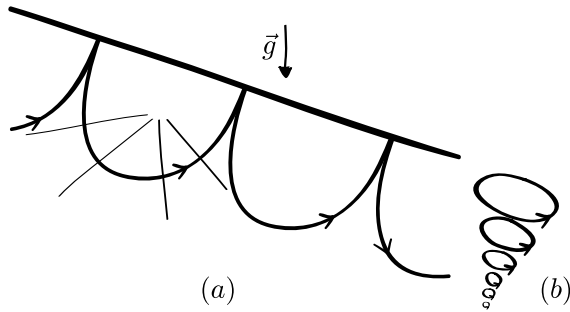
Figure 15. Principles of guided acoustic waves in granular media under gravity. (*a*) Representation of a guided mode in the geometrical acoustics approximation. As the speed of sound increases in depth, the wavefronts (thin lines) are deflected towards the free surface. Take care that the rays represent conventionally plane waves (thin lines): the vibration therefore takes place everywhere, not only in the vicinity of the rays. A guided mode corresponds to a phase matching between waves reflected several times at the free surface and brought to the surface by the gradient in the speed of sound. (*b*) Motion of grains in a guided mode of order 1.

modes that correspond, in terms of geometrical acoustics, to a return of the acoustic ray at the surface with a coherent phase (a phase lag multiple of 2π). It was shown independently by Bonneau *et al* [4, 20, 21] and Gusev *et al* [49, 58] that the dispersion relation satisfies the scaling law

$$\omega \simeq n^{1/6} \, g^{1/6} \left(\frac{E}{\rho} \right)^{1/3} k^{5/6} \qquad (15)$$

where n is the order of the mode. The mode labelled n penetrates sand over a depth of about n times the wavelength λ. Consequently, the characteristic pressure is on the order of $\rho g n \lambda$. Using the scaling law (14) governing the wave velocity, one obtains the above dispersion relation. The propagation is thus slightly dispersive. Furthermore, the different branches of this dispersion relationship are extremely close to each other (varying as $n^{1/6}$) so that a pulse emitted into a granular medium under gravity leads to a multitude of modes propagating at speeds that are relatively close.

The existence of these modes guided by the gravity index gradient was proved experimentally by Bonneau *et al* [21] and by Jacob *et al* [58]. Figure 16 shows, for instance, the propagation of a mode $n = 1$ wave packet, isolated experimentally. The ratio of the phase velocity to the group velocity directly confirms the exponent of the dispersion relation (15) in the limit of low pressure. The existence of multiple elastic modes guided by the index gradient was recovered by Andreotti [4] on a booming dune and later by Vriend and collaborators [107]. Using multiple sensors, Vriend *et al* successfully reconstructed the profile of the speed of sound (figure 14) by analysing the propagation of the different modes. Surprisingly, these authors claim that the multiple modes result from dune layering (see below), although their data clearly show the existence of multiple guided modes in the absence of any index discontinuity [56, 108].

4.5. Modes guided by dune layering

From the previous arguments, one expects the speed of sound to increase continuously with depth, due to gravity. It has been
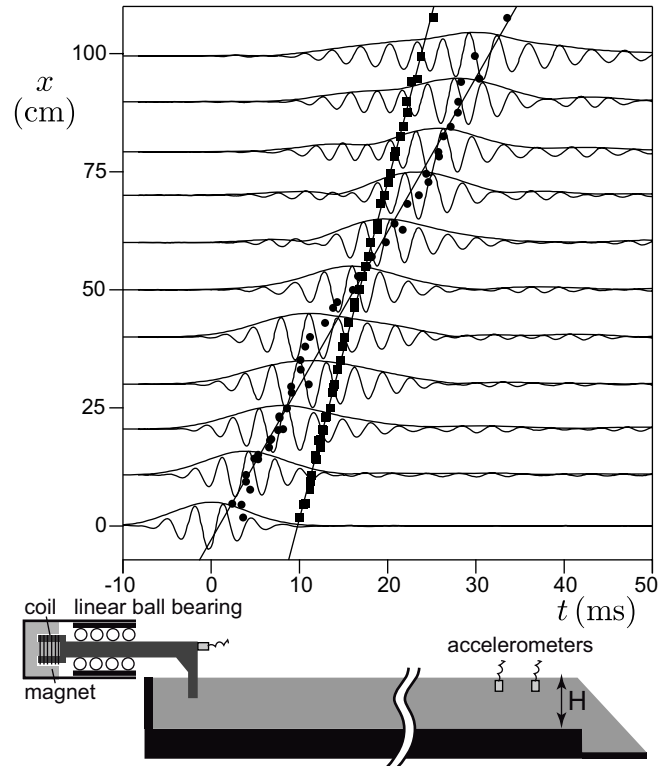

Figure 16. Bottom: experimental set-up used in the lab to show the propagation of modes guided by the gravity-induced index gradient. Top: space–time diagram showing the wave-packet propagation. Starting from the raw signals received at different positions, the wave packet is roughly localized by computing the signal envelope. Then, a local fit by a Gaussian wave packet allows one to determine the centre of the wave packet (●) and its phase with respect to the source (symbols ■ show the space–time coordinates of an iso-phase event). The best fit (thin lines) allows one to extract the group and phase velocities. Measurements performed by Bonneau *et al* [21].

hypothesized by Vriend *et al* [107] that the speed of sound may present discontinuous variations across the interfaces between sedimentary layers. Indeed, as is well known in stratigraphy (cross-bedding), propagative dunes generically present a layered structure parallel to the avalanche slip face. From the acoustic point of view, one mostly expects an effect of humidity, which strongly enhances acoustic dissipation and also increases the speed of sound. Although this may sound surprising initially, most desert sand dunes are filled with water trapped by capillary forces.

Figure 17 schematically shows the influence of such an interface at a depth D below the free surface. At this interface, a fraction of elastic waves are reflected and the remaining is refracted. As the free surface totally reflects waves, this structure again constitutes a wave guide (like Love modes) which is superimposed on that induced by gravity. Let us first neglect the index gradient induced by the pressure field. Modes guided by the interface correspond to a phase coherence of acoustic rays successively reflected by the two interfaces. In the special case where the rays are normal to the interface (figure 17(*a*)), the guided mode corresponds to a standing wave, i.e. a mode of vanishing wave number k. The frequency f_R of this particular mode corresponds to an acoustic resonance of the system. In order to clarify the meaning and the origin of
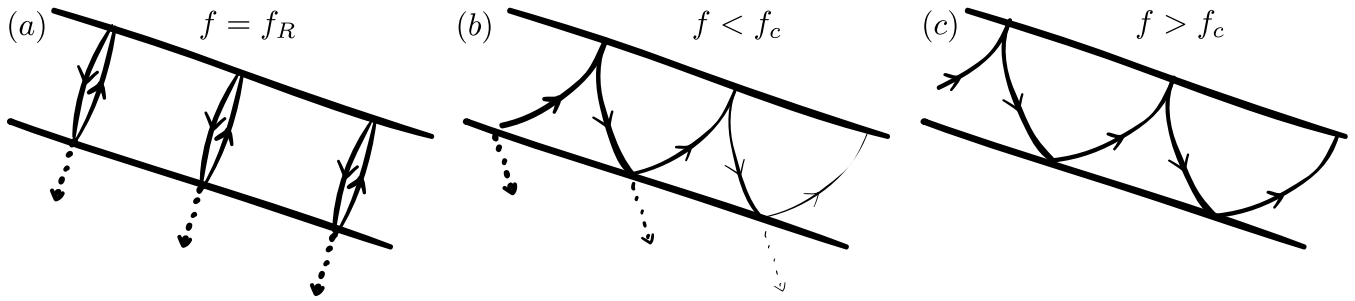
16

Figure 17. Schematic showing the influence of dune layering on elastic wave propagation. The lines correspond to acoustic rays, which represent plane waves. (*a*) Standing resonant mode at the frequency f_R. (*b*) Evanescent mode below the critical frequency f_C. (*c*) Above f_C, the internal reflection of elastic waves ensures that the energy of the elastic mode remains confined in the layer.

this resonance, consider an experiment in which seismic energy is locally injected into the system at a frequency f. When f is close to f_R, the energy does not propagate and is stored. Therefore, the vibration amplitude presents a maximum at $f = f_R$. The tendency of the system to oscillate with a larger amplitude when f is around f_R is, by definition, called a resonance. The sharpness of the resonance is limited by refraction and by damping.

Beyond the resonant frequency f_R, guided modes are propagative. However, the refraction into the lower half-space leads to an energy leak. The waves are thus evanescent, i.e. they decay exponentially in space (figure 17(*b*)). The rays' incidence angle on the interface increases with f and reaches the critical angle at $f = f_C$. Above f_C, total internal reflection of elastic waves occurs. The layer then acts as a wave guide which confines energy. Instead of decaying exponentially in space, above f_C the vibration amplitude decays as the inverse of the square root of the distance to the source. Importantly, f_C is not a resonance since it does not correspond to a frequency at which the system response presents a maximum. f_C is a cut-off frequency above which the frequency response is flat.

4.6. Non-elastic waves

A fundamentally different type of wave has been proposed by Bagnold in the context of booming dunes [9]. From dimensional analysis, assuming that rheology is local [3, 44], the pressure in a granular flow must depend on the shear rate $\dot{\gamma}$ as

$$P = \rho f(\phi) \dot{\gamma}^2 d^2 \qquad (16)$$

where $f(\phi)$ is, at least in the dense regime, a decreasing function of the volume fraction ϕ. By contrast with the elastic waves discussed above, which result from the deformation of the elastic skeleton, non-elastic waves would result from the dynamic compressibility of the granular packing, i.e. the variation of P with ϕ. They would still exist in the limit of hard spheres. Following dimensional analysis, their propagation speed would be much lower than that of elastic waves:

$$c \propto \dot{\gamma} d. \qquad (17)$$

As the effective viscosity scales on $d^2 \dot{\gamma}$, propagation would only be possible at frequencies much smaller than $\dot{\gamma}$.

The existence of these non-elastic waves inside dense granular flows is rather speculative. In the dilute case, however,

the dispersion relation of these waves has been derived [2] from granular kinetic theory, which takes grain inelasticity into account [46, 51]. Experimentally, the speed of sound has been measured in a gaseous granular flow past an obstacle, by analysing the formation of supersonic shock waves [2]. The order of magnitude and the dependence of c with volume fraction ϕ were successfully tested against kinetic theory.

Let us consider the origin of putative non-elastic waves inside an avalanche. If the medium dilates (i.e. if ϕ decreases), the pressure drops so that the grains fall down due to gravity. In turn, this reduces ϕ with a delay, due to inertia. There is thus a non-elastic wave propagation transverse to the avalanche. Using the local rheology assumption [44], one obtains the scaling law followed by the speed of non-elastic waves in that case: $c \propto \sqrt{gH}$. This expression is similar to the velocity of surface gravity waves in shallow water. For a typical avalanche, c would be between 0.1 and $1 \, \text{m s}^{-1}$—order of magnitude found in [2]. The resonant frequency of these waves across the avalanche would scale as $\sqrt{g/H}$ and can be estimated to be 10 Hz. Using reasoning at the scale of the grain that we were not able to follow or reproduce, Bagnold has obtained the scaling law $f \propto \sqrt{g/d}$ for this resonant frequency.

5. Acoustic emission mechanism

In this section, we review the dynamical mechanisms that have been proposed to explain sonic sands.

5.1. Passive resonance

Booming dunes. The simplest possible mechanism is a resonance of the dune. Here, resonance is understood as a maximum of the dune vibration amplitude at a particular frequency f_R. The idea here is that the dry surface layer constitutes a resonant cavity. The standing mode associated with this layer is a passive resonance because energy does not propagate and get stored in the cavity.

Following this idea, the avalanche must be considered a source of noise which injects energy into the static dune over a broad frequency band. The dune would behave as a passive filter which selectively reinforces the frequency f_R. This idea is very clear and suggests straightforward tests detailed below. However, an important source of confusion in the literature
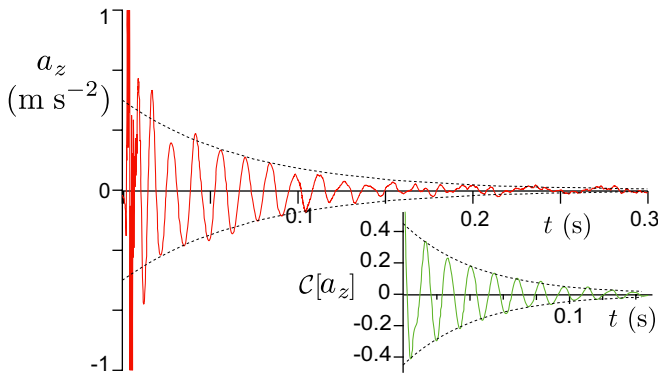
Figure 18. The Makhnovist drum experiment: response of the booming dune to a normal tap constituting a broadband excitation. After the propagative, excited modes have left, the resonant mode, i.e. the standing mode stays. The tail following the tap contains a well-defined frequency that can be interpreted as the first compression resonant mode. Inset: auto-correlation function of the signal shown. The resonant frequency is $f_R \simeq 73$ Hz for these particular conditions of field measurements, while the booming frequency is around 100 Hz. The wet sand layer is at a depth around $D = 50$ cm below the surface. Measurements performed by Bonneau *et al* [20].

comes from the claim that the cut-off frequency f_C, associated with the dry sand layer at the surface of the dune, is a resonant frequency [56, 107, 108]. As detailed above, it is not [6]. The issue is not the incorrect use of the word 'resonance' but the fact that the dune has strictly no reason to pick up the cut-off frequency f_C, as the system behaves like a high-pass filter, not like a band-pass filter. There is no maximum vibration amplitude at the cross-over frequency of such a filter.

Tests. If booming results from a passive resonance of the dune, the booming dune frequency should match the resonant frequency f_R. We have systematically tested this point in the Atlantic Sahara. Most of the time, no resonance can be heard. Figure 18 shows a case where a resonance of the static dune can clearly be identified. The difference between the booming frequency and the resonant frequency was well outside error bars. This is confirmed by the measurements performed Vriend *et al* [107]. They systematically observed the propagation of waves at the booming frequency. Therefore, the booming frequency does not correspond to a resonant standing mode. If booming results from a passive resonance of the dry surface layer of the dune, the vibration mode should match the shape of a resonant mode. Moreover the vibration should be mostly an incoherent noise inside the avalanche. However, the maximum of coherent vibration is located inside the avalanche and the vibration amplitude strongly decreases across the avalanche/dune interface.

The report of an acoustic emission continuing several minutes after the avalanching of sand has ceased is obviously in favour of an explanation of the phenomenon by a passive resonance. We thus refer the reader to the previous discussion of this point and we conclude again that this statement should not be accepted as fact. Note finally that the reproduction of the phenomenon in the lab, without any dune, may be considered as proof in itself that booming avalanches do not result from

a passive resonance. On the basis of this long series of tests, our conclusion is that this hypothesis must indeed be rejected.

Squeaking beaches. By contrast, the frequency of emission f in the impacting pestle experiment (figure 10) nicely corresponds to the natural vibration frequency f_0 of an harmonic oscillator: the mass is the pestle and the spring is the sand below it. The very low elastic modulus of sand explains the order of magnitude of the resonant frequency. In this simple picture, shear bands would play a minor role.

Tests. In order to test this idea, the response of a static pestle, dug into the sand, to an external vibration must be obtained and the resonant frequency f_R compared with the spontaneous emission frequency f.

5.2. Stick–slip instability

A different mechanism previously invoked results from the hysteresis of the friction coefficient μ, defined as the ratio of the shear stress to the normal stress. One can hypothesize that μ decreases from its static value μ_s to its dynamic value μ_d as the shear rate $\dot{\gamma}$ increases from 0 to a value $\dot{\gamma}_d$ which may depend on pressure. This branch of the constitutive relation is obviously unstable as friction decreases when the velocity increases, which results in an even higher velocity. For $\dot{\gamma}$ above $\dot{\gamma}_d$, friction increases and a stable situation is recovered. In a stress-driven flow, this effect leads to the localization of shear stress into a shear band separating a static region ($\dot{\gamma} = 0$) from a moving region ($\dot{\gamma} > \dot{\gamma}_d$).

The generic stick–slip instability occurs when a frictional system is driven into motion at a constant speed V, through a coupling spring or any equivalent restoring mechanism. The inertia of the system and the spring constant allow one to define the length ℓ needed to load the system to the static threshold μ_s, starting from the dynamical threshold μ_d, and the frequency f_0 of the oscillator. At low driving speeds, the time needed to load the system is much larger than the time during which it moves. The frequency f at which the system oscillates therefore scales as ℓ/V. At large driving speeds, the frequency is limited by the frequency f_0 of the oscillator.

It has been proposed by Mills and Chevoir [76] that stick–slip could be the mechanism producing seismic vibrations in booming avalanches, the restoring force being gravity. In order to explain the order of magnitude of the emitted frequency f, this instability would occur at a spatial length scale d, so that the frequency f would scale as $\sqrt{g/d}$. A stick–slip phenomenon can indeed be observed in avalanches driven at a constant flow rate or in plow experiments. However, it takes place at the scale of the avalanche itself so that the pulsation frequency is much lower than acoustical frequencies. It is difficult at this early stage of theoretical development to propose further experimental tests of this idea.

In the rotating pestle experiment, both stick–slip and booming can occur at the same time, which shows their difference of nature. In the plow experiment, which is driven at a controlled velocity V, the expected proportionality of the frequency f with V^{-1} was never observed. Finally, in the impacting pestle experiment, stick–slip is associated with the formation of multiple shear bands but the number of slip
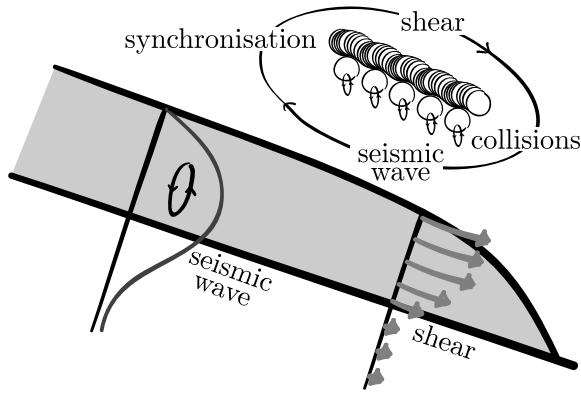
Figure 19. Schematic of the synchronization instability based on the interaction between an elastic wave and granular collisions. The unstable mode is a combination of an elastic wave and the probability that a granular collision occurs in phase with the vibration. Synchronized collisions reinforce vibration. In turn, vibration increases the fraction of synchronized collisions.

layers does not correspond to the number of periods in the emitted signal. Still, in that case, the emission frequency corresponds to the frequency f_0 of the oscillator constituted by the pestle (mass) and the sand grains (spring). Our conclusion is that the stick-slip phenomenon does not explain much of the observations.

5.3. Synchronization instability

The third possible mechanism invoked to explain booming dunes was initially proposed by Poynting and Thomson [91]. It is based on the idea that the avalanche needs to dilate to flow [95]. Considering the motion of a single grain at the surface of an array of grains, dilation and collision occur on average at a frequency $\dot{\gamma}$ [4, 5, 23]. It is then tempting to associate the emission frequency f with the collision frequency $\dot{\gamma}$.

It was first noticed by Andreotti [4] that millions of grains making individual collisions around the same frequency $\dot{\gamma}$, but with a random phase, would not lead to a harmonious sound, but to a noise. This noise can be perfectly heard in the rotating pestle experiment, below the instability threshold. To obtain a coherent sound at a frequency $f \simeq \dot{\gamma}$, the grain collisions must be partly synchronized. This raises two questions. *What is the nature of the coupling signal transmitted to the grains to synchronize them on a large enough scale? What is the dynamical mechanism leading to the grain synchronization?*

Reasoning on the motion of a single grain, Andreotti [4] has shown that a coherent elastic wave can partly synchronize the grain collisions (figure 19). Indeed, when subjected to a vibration, the grains inside the shear layer tend to synchronize with this vibration. In other words, the probability $\mathcal{P}(\phi)$ of observing a phase ϕ between collision and vibration is not a constant, independent of ϕ, but presents a peak around $\phi = 0$ which increases with the vibration amplitude $\mathcal{A}$. More and more grains get synchronized as the vibration amplitude increases. We now come to the positive feedback mechanism, which explains the coherent vibration. Each collision between two grains deform these grains. A fraction

of the translational kinetic energy is thus transferred to the elastic energy stored inside the grains. Then, this energy is radiated and dissipated. The acoustic signal emitted during this elementary event can be decomposed into acoustic modes. As previously remarked, some of these modes are localized and involve only a few grains. Some other modes have a large scale coherence and correspond to the effective medium response. Therefore, a fraction of the translational energy is transferred to coherent acoustic modes at the frequency $\dot{\gamma}$. If the probability $\mathcal{P}(\phi)$ is perfectly flat ($\mathcal{P}(\phi) = 1/2\pi$), there is a negative interference of the contributions of the different grains. The resulting amplitude of vibration is thus null ($\mathcal{A} = 0$). As soon as a fraction (even infinitesimal) of the collisions are synchronized, these collisions reinforce the vibration in phase, coherently (figure 19). This feedback loop can be expressed more formally. The growth rate of the vibration $\mathrm{d}\mathcal{A}/\mathrm{d}t$ due to collisions is proportional to $\int \mathcal{P}(\phi) \exp(\mathrm{i}\phi) \, \mathrm{d}\phi$, which is an increasing function of $\mathcal{A}$. This leads to a linear instability where the amplitude of the coherent acoustic mode and the fraction of synchronized grains grow exponentially in time. This stimulated acoustic emission which synchronizes collision possesses a similarity to a laser.

The synchronization instability allows one to interpret many observations, but not all. It is consistent with the observation that the sand surface emits sound in the air like the membrane of a loud speaker [4]. It explains the saturation of the sound amplitude by the loss of the synchronization power when the grains take off. This instability also presents two thresholds [20]. As vibration is damped, there is a first instability threshold controlled by the dissipation time scale: to get an instability, energy gain due to the partial synchronization of collisions must be larger than energy loss. The second threshold results from the assumption that coherent elastic waves can propagate in the system. For this, the height of dry sand must be sufficiently large (figure 17), as observed in the plow experiment (figure 7).

The synchronization instability was revisited by Douady *et al* [39], with a different perspective on the instability threshold. The claim is that the synchronization only takes place if the coupling wave propagates across the flowing layer height H faster than the duration between two collisions. The instability threshold is thus given by the condition $H = c/\dot{\gamma}$. As the product $\dot{\gamma}H$ is the flow velocity V, this argument predicts a threshold controlled by the ratio V/c. As the minimal velocity V needed to obtain booming would be lower than $1 \, \mathrm{m \, s^{-1}}$, the propagation speed of the coupling wave would also be lower than $1 \, \mathrm{m \, s^{-1}}$, which is not consistent with elastic waves. Although Douady *et al* [39] do not discuss the precise nature of this low-velocity coupling wave, it turns out that Bagnold's non-elastic waves nicely match the requirements. In particular, as they propagate across the layer at a speed $c \propto \sqrt{gH}$, the parameter controlling the instability becomes the Froude number $V/\sqrt{gH}$, as observed in the plow experiment (figure 7).

A third variant of the synchronization instability was proposed by Dagois-Bohy [34]. It assumes shear localization and relates booming to the cooperative motion inside shear bands (figure 20). Transient clusters are synchronized by the
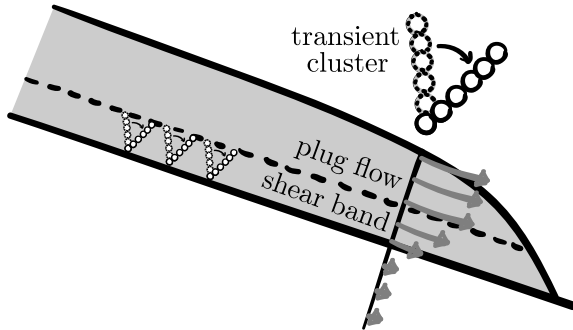
Figure 20. Schematic of the synchronization instability based on the cooperative motion inside shear bands.

fact that they push on the same solid block (the plug flow above the shear band). The coherence of the acoustic emission is then controlled by the length over which the avalanche behaves like a solid.

Tests. Each version of the synchronization instability presents specific aspects that may be tested. The common prediction is the relation between the emission frequency f and the shear rate $\dot{\gamma}$, which is also the mean collision frequency. The key test is thus to simultaneously measure these two quantities. The rotating pestle experiment presented in figure 9 is the only situation in which such measurements have been performed; in this case at least, there is a two decade discrepancy between f and $\dot{\gamma}$. In the linear plow experiment, there are strong indications that shear is localized in a layer whose thickness scales on the grain diameter d. This means that $\dot{\gamma}$ scales on V/d, which does not match the dependence of f, which takes the form $f = f_0 + \alpha V/H$. In the case of gravity-driven avalanches, the hypothesis of an identity $f = \dot{\gamma}$ whatever H and V would require the presence of a wide shear band whose thickness adapts to keep $\dot{\gamma}$ constant. There is no known reason for why this would be the case. Finally, how to explain, for certain dunes like Al Ashkharah (J'alan) [34], that the emission spectrum presents several frequencies f while there is no such possibility for $\dot{\gamma}$. Although not definitive, our conclusion is that this hypothesis must be set aside, unless one succeeds in performing simultaneous measurements of f and $\dot{\gamma}$ showing that they are related.

5.4. Amplification of elastic waves by a sliding frictional interface

The last explanation is based on a theory that assumes the localization of shear in a band separating the avalanche from the static dune [7]. Then, the system is similar to two elastic blocks sliding with friction, one over the other. The picture of a booming avalanche is then very similar to the sand organ experiment, with two noticeable differences: the upper and lower boundary conditions are a free surface and an almost semi-infinite static sand pile, respectively. The key effect was identified by Nosonovsky and Adams [81] and by Caroli and Velicky [27], who showed that an acoustic wave can be amplified coherently when reflected on a sliding frictional interface. Indeed, with the system being open, the

energy of the incident plane wave is no longer conserved, the work of the external driving force being partitioned between frictional dissipation and gain of coherent acoustic energy. A large value of the friction coefficient thus favours energy gain. Therefore, the avalanche behaves as a wave guide whose boundary presents an anomalous reflection. As in a laser, the combination of a cavity with an acoustic amplifier results in a spontaneous emission of coherent waves, if the energy loss is sufficiently low.

Contrary to previous explanations, this effect can be formalized theoretically into a well-posed problem, with one central hypothesis: the avalanche is described as a plug flow of thickness H separated from the static part of the dune by an infinitely small frictional shear band. Under this assumption, the linear stability analysis of a uniform flow can been performed, whose predictions are the following [7].

- The steady homogeneous avalanche is unstable towards elastic waves amplified by friction, above a threshold which compares the dissipation time with the time needed for a wave to propagate across the avalanche thickness H.
- The dispersion relation shows several maxima of the growth rate with very close frequencies. In all these modes, vibration is localized inside the avalanche and drops by a large factor across the shear band. The first mode presents a vibration node at mid-avalanche height; the second mode presents two vibration nodes, etc.
- Close to the threshold, all the unstable modes propagate up the dune. The instability is thus convective and leads to the spatial amplification of a doublet whose frequency scales with the inverse of the dissipation time.
- Far above the threshold, downward propagating modes get amplified as well: the instability becomes absolute. The frequencies associated with the maxima of the growth rate scale as c/H, where c is the speed of sound under a pressure $\rho g H$.

This theory predicts and allows one to understand a large part of the phenomenology of booming avalanches.

- Emission takes place around a well-defined frequency, but with a tremolo that results from the superposition of different modes (two at least) (figure 5).
- As the instability is convective, the vibration amplitude is amplified exponentially in space, from the tip of the avalanche to its core (figures 4 and 6).
- The emission frequency f is selected at the front of the avalanche, around the place where the height H crosses the threshold height H_{th}. f is thus not very sensitive to the shape of the avalanche (figure 3).
- Sonic sands are not special except for their large friction coefficient, as the amplification results from friction.
- Since the instability is limited by acoustic dissipation, humidity increases the emission threshold.
- Vibration is localized inside the avalanche and drops by a factor of ten when crossing the interface between the avalanche and the dune. It presents a node at mid-avalanche height (figure 6)
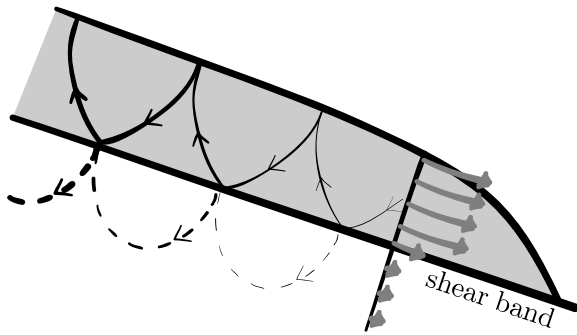
20

Figure 21. Schematic showing the amplification of guided elastic waves by reflection on the frictional interface separating the avalanche from the dune.

Rather than entering the mathematical details, we will describe here the principle of the instability mechanism in terms of acoustic rays (figure 21). As shown in [27, 81], the reflection of elastic waves on the frictional interface results in energy pumping from shearing motion to coherent acoustic waves. The maximum energy gain and thus the maximum growth rate is obtained for a particular angle of incidence. As the wave speed depends only on z, this condition determines a single ray, whatever the wave number k. In the geometric acoustics approximation (figure 21), guided modes are selected by the condition of constructive interference between plane waves as they bounce back and forth. Altogether, there is a local maximum of the growth rate periodically in kH, for each constructive interference. As in the sand organ experiment, geometry selects the most amplified wave number.

Obtaining the corresponding frequencies f is then a non-trivial issue. One needs to calculate normal modes using continuum mechanics instead of using geometrical acoustics [7]. Moreover, one needs to know both the acoustic dissipation and the speed of sound c. The results of the sand organ experiment show that c can be significantly different from the expectation.

Tests. This theory is based on an idealized picture of granular avalanches. However, even with shear band localization, the granular motion is never a pure solid block motion, but rather presents a diffuse shear profile. The persistence of the amplification mechanism in that case requires two properties that may be tested experimentally or numerically. First, transverse waves should be able to propagate through a granular layer fluidized by a shear band. In other words, granular material must be visco-elastic close to jamming. Second, the shear stress in a granular flow must nonetheless increase with static pressure P but also be modulated by the acoustic pressure p. In other words, the same frictional behaviour must exist at the time scale of shear $\dot{\gamma}^{-1}$ and at the time scale of elastic waves f^{-1}. Provided that the shear stress (or equivalently the viscosity) increases with the total pressure $P + p$, acoustic modes get coupled to the mean flow and can consequently be amplified when reflected by the (diffusive) shear band [43]. An important theoretical test would be to perform the linear stability analysis of a flowing visco-elastic material presenting a frictional behaviour.

One of the strong, yet not verified, predictions of this theory is the selective amplification of up-slope propagating waves. This test is very easy to perform in the sand organ experiment, as there is a single unstable mode. In the case of booming dunes, one expects several unstable modes to be superimposed, which makes the analysis more difficult to perform. Indeed, in that case, one cannot simply use the phase lag between two points of measurement, as done in [22, 33].

Although the principle of the instability—a cavity bordered by a shear band amplifying elastic waves, thanks to friction—is general, it must be carefully adapted to each geometry to obtain reliable predictions. In the sand organ experiment, this dynamical mechanism is validated by several experimental characteristics (figure 12): the sound emission results from a convective instability; the exponential amplification of upward propagating waves is directly observed; the wavelength scales on the tube radius. Contrary to booming avalanches, the laboratory geometries (plow experiment, rotating pestle experiment and jar experiment) are characterized by an aspect ratio L/H of order 1. Therefore, the instability cannot be convective and the cavity length L should play an important role. It is reasonable to think that these three experiments present a bounding shear band that may amplify elastic waves. Experimental results are consistent with a selection of the emission frequency f by the speed of sound c and the sand pile geometry. In the plow experiment, the selected frequency f decreases typically as the inverse of the moving sand length L (figure 8); in the jar experiment, f decreases with the thickness H (figure 11); in the rotating pestle experiment, f does not depend on the shear rate $\dot{\gamma}$ but increases with the applied pressure, which controls c (figure 9). To achieve a complete validation, the linear stability analysis must be performed case by case, in these confined geometries.

6. Perspectives

Given the degree of controversy, a simple conclusion would not be appropriate for the subject we have treated. Rather, we would like to indicate possible future directions of research.

- We have emphasized throughout this review that experimental tests are the only way to solve controversies. Most results presented in this review need to be reproduced independently to establish a base of consensual facts.
- A correct understanding of sand rheology close to the jamming transition is still lacking. In particular, the direct measurement of the velocity profile inside an avalanche remains a major issue.
- Direct numerical simulations using discrete element methods have proved their usefulness in understanding the mechanical behaviour of granular matter. The numerical reproduction of a spontaneous acoustic emission induced by a granular shear flow would certainly help to analyse the phenomenon in detail.
- One of the important aspects of the problem is the fact that, due to friction, the compressibility of the material cannot be neglected at a low Mach number, as it is coupled to the shear flow. The principle of acoustic wave amplification

can probably be generalized and further applied to any thick interface inside which the shear stress increases with pressure [43]. For instance, one can wonder if instabilities observed in microfluidic flows of concentrated colloidal suspensions [57] could originate from the same fundamental mechanisms as sonic sands.

- The central issue of sonic sands is to understand how a steady flow at a low Mach number can generate acoustic waves. The reverse problem also looks promising. *How do vibrations affect a mean granular shear flow?* In particular, mechanical fluctuations in disordered athermal systems could be a source of noise analogous to temperature in thermal systems [94] activating motion below the jamming point.

Acknowledgments

References

[1] Allard J F 1993 Propagation of sound in porous media *Modelling Sound Absorbing Materials* (London: Elsevier)
[2] Amarouchene Y and Kellay H 2006 Speed of sound from shock fronts in granular flows *Phys. Fluids* **18** 031707
[3] Andreotti B, Forterre Y and Pouliquen O 2011 Granular matter, between solid and fluid *EDP Science* (Cambridge: Cambridge University Press) (in French)
[4] Andreotti B 2004 The song of dunes as a wave-particle mode locking *Phys. Rev. Lett.* **93** 238001
[5] Andreotti 2007 A mean field model for the rheology and the dynamical phase transitions in the flow of granular matter *Europhys. Lett.* **79** 34001
[6] Andreotti B, Bonneau L and Clement E 2008. Comment on 'Solving the mystery of booming sand dunes' by Nathalie M Vriend *et al*, *Geophys. Res. Lett.* **35** L08306
[7] Andreotti B and Bonneau L 2009 Booming dune instability *Phys. Rev. Lett.* **103** 238001
[8] Bagnold R A 1941 *The Physics of Blown Sand and Desert Dunes* (London: Methuen)
[9] Bagnold R A 1966 The shearing and dilatation of dry sand and the 'singing' mechanism *Proc. R. Soc. Lond.* A **295** 219–32
[10] Ball P 2007 The dune chorus *Nature* **449** 10
[11] Baumberger T, Berthoud P and Caroli C 1999 Physical analysis of the state- and rate-dependent friction law: II. Dynamic friction *Phys. Rev.* B **60** 3928
[12] Bertho Y, Giorgiutti-Dauphiné F, Raafat T, Hinch E J, Herrmann H J and Hulin J-P 2002 Powder flow down a vertical pipe: the effect of air flow *J. Fluid Mech.* **459** 317–45
[13] Bertho Y, Brunet Th, Giorgiutti-Dauphiné F and Hulin J-P 2004 Influence of humidity on granular packings with moving walls *Europhys. Lett.* **67** 955
[14] Beverloo W A, Leniger H A and van de Velde J 1961 The flow of granular solids through orifices *Chem. Eng. Sci.* **15** 260–9
[15] Bollaert W 1851 Observations on the geography of southern Peru *J. R. Geogr. Soc. Lond.* **21** 99–130
[16] Bolton H C and Julien A A 1884 Musical sand, its wide distribution and properties *Am. Assoc. Adv. Sci.* **33** 408–13
[17] Bolton H C and Julien A A 1888 The true cause of sonorousness in sand *Trans. N. Y. Acad. Sci.* **8** 9–10

[18] Bolton H C 1889 Researches on sonorous sand in the Peninsula of Sinai *Proc. Am. Assoc. Adv. Sci.* **38** 137–59
[19] Bolton H C 1890 Researches on musical sand in the Hawaiian Islands and in California *Trans. N. Y. Acad. Sci.* **10** 28–35
[20] Bonneau L, Andreotti B and Clement E 2007 Surface elastic waves in granular media under gravity and their relation to booming avalanches *Phys. Rev.* E **75** 016602
[21] Bonneau L, Andreotti B and Clement E 2008 Evidence of Rayleigh–Hertz surface waves and shear stiffness anomaly in granular media *Phys. Rev. Lett.* **101** 118001
[22] Bonneau L, Catelin-Jullien T and Andreotti B 2010 Friction induced amplification of acoustic waves in a low Mach number granular flow *Phys. Rev.* E **82** 011309
[23] Brown A E, Campbell W A, Jones J M and Thomas E R 1964 Musical sand: the singing sands of the seashore: II *Proc. Univ. Newcastle Upon Tyne Phil. Soc.* **1** 1–21
[24] Brunet Th, Jia X and Mills P 2008 Mechanisms for acoustic absorption in dry and weakly wet granular media *Phys. Rev. Lett.* **101** 138001
[25] Burton R F 1879 Itineraries of the second Khedivial expedition *J. R. Geogr. Soc. Lond.* **49** 1–150
[26] Caroli C and Velicky B 2002 Pressure dependence of the sound velocity in a two-dimensional lattice of Hertz–Mindlin balls: mean-field description *Phys. Rev.* E **65** 021307
[27] Caroli C and Velicky B 2003 Anomalous acoustic reflection on a sliding interface or a shear band *Phys. Rev.* E **67** 061301
[28] Carus-Wilson C 1888 Musical sand *Bournemouth Soc. Nat. Sci.* **2** 1–20
[29] Carus-Wilson C 1891 The production of musical notes from non-musical sands *Nature* **44** 322–23
[30] Carus-Wilson C 1908 Musical sands *Nature* **77** 222
[31] Criswell D R, Lindsay J F and Reasoner D L 1975 Seismic and acoustic emissions of a booming dune *J. Geophys. Res.* **80** 4963–74
[32] Curzon G 1923 Singing sands *Tales of Travel* (London: Century) pp 261–339
[33] Dagois-Bohy S, Ngo S, Courrech du Pont S and Douady S 2010 Laboratory singing sand avalanches *Ultrasonics* **50** 127–32
[34] Dagois-Bohy S 2011 *PhD Thesis* Université Paris-Diderot
[35] Daraio C, Nesterenko V F, Herbold E B and S J 2006 Tunability of solitary wave properties in one-dimensional strongly nonlinear phononic crystals *Phys. Rev.* E **73** 026610
[36] Darwin C 1835 Northern Chile and Peru *The Voyage of the Beagle* (New York: Dutton) (reprinted in 1979)
[37] Dhoriyani M L, Jonnalagadda K K, Kandikatla R K and Rao K K 2006 Silo music: sound emission during the flow of granular materials through tubes *Powder Technol.* **167** 55–71
[38] Douady S, Andreotti B, Daerr A and Cladé P 2002 The four fronts and the two avalanches *C.R. Phys.* **3** 177–86
[39] Douady S, Manning A, Hersen P, Elbelrhiti H, Protiere S, Daerr A and Kabbachi B 2006 Song of the dunes as a self-synchronized instrument *Phys. Rev. Lett.* **97** 018002
[40] Doughty C M 1888 *Travels in Arabia Deserta* vol 1 (Cambridge: Cambridge University Press) pp 307–8
[41] Duffy J and Mindlin R D 1957 Stress–strain relations and vibrations of a granular medium *J. Appl. Mech.* **24** 585
[42] Elbelrhiti H, Andreotti B and Claudin P 2008 Barchan dune corridors: field characterization and investigation of control parameters *J. Geophys. Res.* **113** F02S15
[43] Furukawa A and Tanaka H 2006 Violation of the incompressibility of liquid by simple shear flow *Nature* **443** 434–8

[44] Midi G D R 2004 On dense granular flows *Eur. Phys. J.* E **14** 341

[45] Goddard G 1990 Nonlinear elasticity and pressure-dependent wave speeds in granular media *Proc. R. Soc. Lond.* A **430** 105

[46] Goldhirsch I 2003 Rapid granular flows *Annu. Rev. Fluid Mech.* **35** 267–93

[47] Goldsack D, Leach M and Kilkenny C 1997 Natural and artificial singing sands *Nature* **386** 29

[48] Goldsmid F J 1897 Sand dunes in Afghanistan *Geogr. J.* **9** 454

[49] Gusev V E, Aleshin V and Tournat V 2006 Acoustic waves in an elastic channel near the free surface of granular media *Phys. Rev. Lett.* **96** 214301

[50] Haff P K 1979 Booming sands of the Mojave Desert and the Basin and Range Province, California *California Institute of Technology Internal Report* NSF PHY76–83685, Pasadena, CA

[51] Haff P K 1983 Grain flow as a fluid-mechanical phenomenon *J. Fluid Mech.* **134** 401–30

[52] Haff P K 1986 Booming dunes *Am. Sci.* **74** 376–81

[53] Harding King W J 1912 Travels in the Libyan desert *Geogr. J.* **39** 133–37

[54] Huerre P and Monkewitz P P 1990 Local and global instabilities in spatially developing flows *Annu. Rev. Fluid Mech.* **22** 473–537

[55] Humphries D W 1966 The booming sand of Korizo, Sahara, and the squeaking sand of Gower, S Wales: a comparison of the fundamental characteristics of two musical sands *Sedimentology* **6** 135–52

[56] Hunt M L and Vriend N M 2010 Booming sand dunes *Annu. Rev. Earth Planet. Sci.* **38** 281–301

[57] Isa L, Besseling R, Morozov A N and Poon W C K 2009 Velocity oscillations in microfluidic flows of concentrated colloidal suspensions *Phys. Rev. Lett.* **102** 058302

[58] Jacob X, Aleshin V, Tournat V, Leclaire P, Lauriks W and Gusev V E 2008 Acoustic probing of the jamming transition in an unconsolidated granular medium *Phys. Rev. Lett.* **100** 158003

[59] Janssen H A 1895 *Z. Ver. Dtsch. Ing.* **39** 1045

[60] Jia X, Caroli C and Velicky B 1999 Ultrasound propagation in externally stressed granular media *Phys. Rev. Lett.* **82** 1863–6

[61] Job S, Melo F, Sokolow A and Sen S 2005 How Hertzian solitary waves interact with boundaries in a 1D granular medium *Phys. Rev. Lett.* **94** 178002

[62] Job S, Santibanez F, Tapia F and Melo F 2008 Nonlinear waves in dry and wet Hertzian granular chains *Ultrasonics* **48** 506–14

[63] Jop P, Forterre Y and Pouliquen O 2006 A new constitutive law for dense granular flows *Nature* **441** 727

[64] Johnson P A and Jia X 2005 Nonlinear dynamics, granular media and dynamic earthquake triggering *Nature* **437** 871–4

[65] Kilkenny C, Leach M F and Goldsack D E 1997 The acoustic emission of silica gel *Can. Acoust.* **25** 28

[66] Landau L D and Lifshitz E M 1959 *Theory of Elasticity* (Oxford: Pergamon)

[67] Leach M F, Goldsack D E and Kilkenny C 1999 Booming sand as a possible source of single frequency sound *Proc. 6th Int. Congress on Sound and Vibration (Copenhagen, Denmark)* pp 1983–8

[68] Ledoux A E 1920 Singing sands *Science* **51** 462–4

[69] Lenz O 1912 Reise durch Marokko, die Sahara und den Sudan *Geogr. J.* **39** 133–34

[70] Lewis A D 1936 Roaring sands of the Kalahari desert *S. Afr. Geogr. Soc.* **19** 33–49

[71] Lindsay J F, Criswell D R, Criswell T L and Criswell B S 1976 Sound-producing dune and beach sands *Geol. Soc. Am. Bull.* **87** 463–73

[72] Makse H, Gland N, Johnson D L and Schwartz L 2004 Granular packings: nonlinear elasticity, sound propagation, and collective relaxation dynamics *Phys. Rev.* E **70** 061302

[73] Makse H, Gland N, Johnson D L and Schwartz L 1999 Why effective medium theory fails in granular materials *Phys. Rev. Lett.* **83** 5070

[74] Maupassant G 1882 La peur *Les Contes de la Bécasse (Journal Le Gaulois)*

[75] Miller P 1956 *Errand into the Wilderness* (Cambridge, MA: Belknap Press of Harvard University Press)

[76] Mills P and Chevoir F 2009 Rheology of granular materials and sound emission near the jamming transition *AIP Conf. Proc.* **1145** 511–4

[77] Miwa S, Hidaka J and Shimosaka A 1983 Musical sand, powder science and technology in Japan *KONA* **1** 64–72

[78] Miwa S, Ozaki T and Kimura M 1995 Evaluation of the sound-producing properties of singing sand *Sci. Eng. Rev. Doshisha Univ.* **36** 67–76

[79] Muite B K, Quinn S F, Sundaresan S and Rao K K 2004 Silo music and silo quake: granular flow-induced vibration *Powder Technol.* **145** 190–202

[80] Nishiyama K and Mori S 1982 Frequency of sound from singing sand *Japan. J. Appl. Phys.* **21** 591–5

[81] Nosonovsky M and Adam G G 2001 Dilatational and shear waves induced by the frictional sliding of two elastic half-spaces *Int. J. Eng. Sci.* **39** 1257

[82] Nori F, Sholtz P and Bretz M 1997 Booming sand *Sci. Am.* **277** 84–9

[83] Norris A N and Johnson D L 1997 Nonlinear elasticity of granular media *J. Appl. Mech.* **64** 39

[84] Ovarlez G, Fond C and Clément E 2003 Overshoot effect in the Janssen granular column: a crucial test for granular mechanics *Phys. Rev.* E **67** 060302

[85] Patitsas A J 2003 Booming and singing acoustic emissions from fluidized granular beds *J. Fluids Struct.* **17** 287–315

[86] Patitsas A J 2008 Singing sands, musical grains and booming sand dunes *Sci. J. Int.* **2** 1

[87] Percier B, Manneville S, McElwaine J N, Morris S W and Taberlet N 2011 Lift and drag forces on an inclined plow moving over a granular surface *Phys. Rev.* E **84** 051302

[88] Pétillon P Y 1992 *Histoire de la Littérature Américaine* (Paris: Fayard) pp 1939–89

[89] Polo M 1295 *The Travels of Marco Polo* (New York: Orion) (reprinted in 1958)

[90] Poynting J H 1908 Musical sands *Nature* **77** 248

[91] Poynting J H and Thomson J J 1909 *A Text-book of Physics* vol 2 *Sound* (London: Charles Griffin & Co)

[92] Philby H 1922 *The Heart of Arabia; A Record of Travel and Exploration* (London: Constable)

[93] Qu J, Sun B, Zhang W, Wang Y and Kang G 1995 Surface texture of quartz grain in booming sand and its acoustic significance *Chin. Sci. Bull.* **40** 1719–23

[94] Reddy K A, Forterre Y and Pouliquen O 2011 Evidence of mechanically activated processes in slow granular flows *Phys. Rev. Lett.* **106** 108301

[95] Reynolds O 1885 On the dilatancy of media composed of rigid particles in contact, with experimental illustrations *Phil. Mag.* **20** 469–81

[96] Ridgway K and Scotton J B 1973 Whistling sand beaches in the British Isles *Sedimentology* **20** 263–79

[97] Shaw W B K 1936 An expedition in the southern Libyan desert *Geogr. J.* **87** 193–217

[98] Sholtz P, Bretz M and Nori F 1997 Sound-producing sand avalanches *Contemp. Phys.* **38** 329–42

[99] Somfai E, van Hecke M, Ellenbroek W G, Shundyak K and van Saarloos W 2007 Critical and noncritical jamming of frictional grains *Phys. Rev.* E **75** 020301

[100] Takahara H 1973 Sounding mechanism of singing sand *J. Acoust. Soc. Am.* **53** 634–39

[101] Thomas B 1932 Across the mountainous sands of Uruq-Adh-Dhahiya *Arabia Felix* (London: Cape) pp 164–79

[102] Tournat V, Zaitsev V Y, Nazarov V E, Gusev V E and Castagnede B 2005 Experimental study of nonlinear acoustic effects in a granular medium *Acoust. Phys.* **51** 543–53

[103] Tournat V and Gusev V 2009 Nonlinear coda-type elastic waves in stressed granular media *Phys. Rev.* E **80** 011306

[104] Tournat V and Gusev V 2010 Acoustics of unconsolidated granular media: an overview of recent results and several open problems *Acta Acust.* **96** 208–24

[105] Tschiffely AF 1933 *From Southern Cross to Pole Star* (London: Heinemann)

[106] Vatin J C 1984 Désert construit et inventé, Sahara perdu ou retrouvé: le jeu des imaginaires *Rev. l'Occident musulman et de la Méditerranée* **37** 107–31

[107] Vriend N M, Hunt M L, Clayton R W, Brennen C E, Brantley K S and Ruiz-Angulo A 2007 Solving the mystery of booming sand dunes *Geophys. Res. Lett.* **34** L16306

[108] Vriend N M, Hunt M L, Clayton R W, Brennen C E, Brantley K S and Ruiz-Angulo A 2008 Reply to comment by B Andreotti *et al* on 'Solving the mystery of booming sand dunes' *Geophys. Res. Lett.* **35** L08307

[109] Walton K 1987 The effective elastic moduli of a random packing of spheres *J. Mech. Phys. Solids* **35** 213

[110] Wildea K, Ruckaa M and Tejchman J 2008 Silo music-mechanism of dynamic flow and structure interaction *Powder Technol.* **186** 113–29

[111] Yule H 1866 *Cathay and the Way Thither* (London: Hakluyt Society)